

Longitudinal Auditory Pathophysiology Following Mild Blast Induced Trauma

Emily X. Han^{1,2}, Joseph M. Fernandez^{2,3}, Caitlin Swanberg², Riya Shi^{2,3}, Edward L.
Bartlett^{1,2}

¹Dept. of Biological Sciences, College of Science, Purdue University, West
Lafayette, IN

²Weldon School of Biomedical Engineering, Purdue University, West Lafayette,
IN

³Dept. Basic Medical Sciences, College of Veterinary Medicine, Purdue
University, West Lafayette, IN

Running head: Longitudinal blast auditory pathophysiology

Correspondence should be addressed to Edward Bartlett (ebartle@purdue.edu).

Department of Biological Sciences and

The Weldon School of Biomedical Engineering

206 S. Martin Jischke Dr.

Purdue University

West Lafayette, Indiana 47907-1791

Keywords: Blast, traumatic brain injury, envelope following response, neurodegeneration,

22 auditory evoked potentials

23

24 **Abstract**

25 Blast-induced hearing difficulties affect thousands of veterans and civilians. The

26 long-term impact of even a mild blast exposure on the central auditory system is

27 hypothesized to contribute to lasting behavioral complaints associated with mild

28 blast traumatic brain injury (bTBI). Although recovery from mild blast has been

29 studied separately over brief or long time windows, few, if any, studies have

30 investigated recovery longitudinally over short-term and longer-term (months) time

31 windows. Specifically, many peripheral measures of auditory function either recover

32 or exhibit subclinical deficits, masking deficits in processing complex, real-world

33 stimuli that may recover differently. Thus, examining the acute time course and

34 pattern of neurophysiological impairment using appropriate stimuli is critical to better

35 understanding and intervention of bTBI-induced auditory system impairments. Here,

36 we compared auditory brainstem response, middle-latency auditory evoked

37 potentials, and envelope following responses. Stimuli were clicks, tone pips,

38 amplitude modulated tones in quiet and in noise, and speech-like stimuli (iterated

39 rippled noise pitch contours) in adult male rats subjected to mild blast and sham

40 exposure over the course of two months. We found that blast animals demonstrated

41 drastic threshold increases and auditory transmission deficits immediately after blast

42 exposure, followed by substantial recovery during the window of 7-14 days

43 post-blast, though with some deficits remaining even after two months. Challenging

44 conditions and speech-like stimuli can better elucidate mild bTBI-induced auditory

45 deficit during this period. Our results suggest multiphasic recovery and therefore

46 potentially different time windows for treatment, and deficits can be best observed

47 using a small battery of sound stimuli.

48

49 **New and Noteworthy**

50 Few studies on blast-induced hearing deficits go beyond simple sounds and sparsely

51 track post-exposure. Therefore, the recovery arc for potential therapies and

52 real-world listening is poorly understood. Evidence suggested multiple recovery

53 phases over 2 months post-exposure. Hearing thresholds largely recovered within

54 14 days and partially explained recovery. However, mid-latency responses,

55 responses to AM in noise, and speech-like pitch sweeps exhibited extended

56 changes, implying persistent central auditory deficits and the importance of

57 subclinical threshold shifts.

58 Introduction

59 Hearing loss stands out as one of the most commonly reported consequences
60 following blast injuries and can last for months or even years without significant
61 external injury (Cohen et al. 2002; Cave et al. 2007; Ritenour et al. 2008; Saunders
62 et al. 2015). Most studies regarding blast-induced hearing loss have focused on
63 damage in different parts of the peripheral auditory system (PAS) (Kerr 1980;
64 DePalma et al. 2005), including hair cells, cochlear synapses, and auditory nerve
65 damage. However, significant hearing difficulties can occur in the absence of
66 peripheral diagnostic indicators such as eardrum rupture or clinical threshold shifts
67 (hearing loss >25 dB), indicating potential disruptions upstream (Remenschneider et
68 al. 2014; Saunders et al. 2015; Van Haesendonck et al. 2018).

69 Increasing clinical (Berger et al. 1997; Cohen et al. 2002; Cave et al. 2007; Ritenour
70 et al. 2008; Lew et al. 2009; Gallun et al. 2012a) and laboratory (Patterson and
71 Hamernik 1997; Ewert et al. 2012; Cho et al. 2013b; Du et al. 2013; Masri et al. 2018)
72 findings suggest that the central auditory system (CAS) contains blast-susceptible
73 structures. Subcortical CAS may be particularly vulnerable to blast injury, including
74 mechanical damage and blood-brain barrier (BBB) permeability, excitotoxicity, and
75 elevated markers of oxidative stress and neuroinflammation for at least 2 weeks
76 (Knudsen and Øen 2003; Leung et al. 2008; Säljö et al. 2011; Cho et al. 2013a; Song
77 et al. 2015; Walls et al. 2016). Functional changes, such as hyperactivity in the
78 auditory brainstem (Luo et al. 2014a, 2014b) or structural changes in OHC loss
79 (Ewert et al. 2012) or in the inferior colliculus (IC) and auditory thalamus (Mao et al.

2012), have been shown at 1-2 time points post-blast at various time points up to 2-3 weeks. Understanding the trajectory of post-blast recovery from primary and secondary damage can help to identify critical time points for diagnostics and therapies.

Clinical reports have suspected “hidden hearing loss” in blast-exposed veterans due to deficits in suprathreshold auditory processing with minimal changes in auditory thresholds (Gallun et al. 2012a; Saunders et al. 2015; Bressler et al. 2017) One consequence to this loss could be CAS adaptations to peripheral deafferentation (Caspary et al. 2005, 2008; Wang et al. 2009), which may lead to impaired temporal processing (Walton 2010; Parthasarathy and Bartlett 2011, 2012; Rabang et al. 2012). Blast studies on human subjects often used speech and complex temporally modulated stimuli to pin down “hidden” temporal processing losses at suprathreshold levels (Gallun et al. 2012b; Saunders et al. 2015; Bressler et al. 2017; Kubli et al. 2018). However, blast studies in animals rarely go beyond simple auditory stimuli (Ewert et al. 2012; Race et al. 2017; Masri et al. 2018).

In the current study, in addition to traditional measures, we chose Iterated Rippled Noise (IRN) to create a pitch contour with adjustable salience alongside Amplitude Modulation (AM) stimuli in quiet and in modulated noise as temporally complex stimuli in assessing the processing of temporal attributes. IRN has been used in neurophysiological and behavioral studies in both human (Krishnan et al. 2014, 2015; Peter et al. 2014; Thompson and Marozeau 2014; Wagner et al. 2017) and animal

102 models (Bendor and Wang 2005; Alsindi et al. 2018).

103

104 **Materials and Methods**

105 **Subject**

106 Male Sprague-Dawley rats (3-4 months) were assigned into Sham group and Blast
107 group randomly. A total of 11 Sham animals and 13 blast animals were used in this
108 study. For a given sound stimulus, only complete sets of responses that included all
109 time points were used for analysis. In a few sessions, there were recording sessions
110 contaminated by movement artifact or movements that displaced electrode positions,
111 and response sets affected by those were not included. All animals were kept and
112 raised in relatively quiet and standard laboratory animal housing conditions. All
113 protocols were approved by the Purdue Animals Care and Use Committee (PACUC
114 #1111000280).

115

116 **Blast Exposure**

117 Animals were anesthetized through intraperitoneal injection of a ketamine/xylazine
118 cocktail (80 mg/kg and 10 mg/kg, respectively). The absence of eye-blink and
119 paw-withdrawal reflexes was ensured prior to proceeding. Anesthetized animals
120 were then placed on a platform beneath an open-ended shock tube to be exposed to
121 the blast event, as described in our prior publications (Song et al. 2015; Walls et al.
122 2016; Race et al. 2017).

123

124 For the Blast group, each rat's head was positioned beneath the open end of the
 125 shock tube such that the dorsum of the skull was the incident surface exposed to a
 126 composite blast (shock wave + blast wind). A custom plexiglass housing was
 127 temporarily placed over the animal's torso for body protection to avoid cardiac or
 128 pulmonary effects of blast and to simulate the protective effects of military body
 129 armor (Rafaels et al. 2011). The head was fixed with a stereotaxic head frame with
 130 bite bar and ear bars (Kopf Instruments) to prevent blast wind-induced head
 131 acceleration. The blast exposure exhibited a recorded pressure profile with a rise to
 132 peak pressure within 0.3 msec, followed by overpressure and underpressure periods
 133 as follows: side-on (static) 150 kPa maximum overpressure, 1.25 msec overpressure
 134 duration, and 20 kPa minimum underpressure; face on (dynamic) 160 kPa maximum
 135 overpressure, 1.75 msec overpressure duration, and 5 kPa minimum underpressure.
 136 These conditions were the same as reported in our prior publications (Song et al.
 137 2015; Walls et al. 2016; Race et al. 2017) and are considered to be a mild blast
 138 exposure, given the magnitude of the exposure and its single occurrence. All but one
 139 blast animal survived the exposure without displaying any motor or behavioral deficit
 140 during each animal's longitudinal follow-up period.

141

142 Sham animals were placed equidistant from the blast source, but out of the path of
 143 the shockwave, therefore only exposed to the blast noise. Tympanic membrane
 144 integrity was verified for all Blast and Sham animals after injury using a surgical
 145 microscope.

146 ***(Insert Fig. 1 about here)***

147

148 **Auditory Evoked Potential Recordings**

149 The animals underwent two-channel Auditory Evoked Potential (AEP) recordings at
 150 the following time points: pre-exposure (baseline), 1 day, 4 days, 7 days, 10 days, 14
 151 days, 1 month, and 2 months. While the animals were under 1.8-2% isoflurane
 152 anesthesia, subdermal needle electrodes (Ambu) were inserted in the following
 153 locations (Fig. 1A): Channel 1 positive electrode was placed along the midline of the
 154 head (mid-sagittal) oriented Fz to Cz. Channel 2 positive electrode was positioned
 155 C3 to C4 along the interaural line. The negative/inverting electrode (used with
 156 positive electrodes for both channels 1 and 2) was placed under the mastoid of the
 157 right ear ipsilateral to the speaker. A ground electrode was placed in the back of the
 158 animal. These configurations were consistent with prior publications from our
 159 laboratory (Parthasarathy and Bartlett 2011, 2012; Parthasarathy et al. 2014; Lai and
 160 Bartlett 2015; Lai et al. 2017). Electrode impedances were confirmed to be less than
 161 1 k Ω using a low impedance amplifier (RA4LI, TDT). After electrode placement, we
 162 subsequently sedated the animals by intramuscular injection of 0.2-0.3 mg/kg
 163 dexmedetomidine (Dexdomitor). AEP recordings were performed 10-15 min after
 164 removal from isoflurane to avoid anesthetic effects. The animals could respond to
 165 pain and acoustic stimuli but tend sit calmly under dexmedetomidine sedation,
 166 allowing about 3 hours of recording time.

167

168 Acoustic stimuli were presented free-field to the right ear (90° azimuth) of animals,
169 with directly in front of the animals' face as the reference for 0° azimuth, using a
170 calibrated speaker (Bowers and Wilkins) at a distance of 115 cm directly facing the
171 right ear. The measurements used in this study included auditory brainstem
172 responses (ABRs), middle-latency responses (MLRs), envelop-following responses
173 (EFRs) using AM in noise stimuli, and IRNs.

174

175 ABR and MLR

176 6 Sham animals and 10 Blast animals were used in ABR analysis. For ABR,
177 rectangular clicks (0.1 msec duration) and tone-pips (2 msec duration, 0.5 msec cos²
178 rise-fall time) with frequencies of 8 kHz and 16kHz were used. 8 kHz and 16 kHz
179 were chosen based on previous findings: with 6-16 kHz being the most sensitive
180 hearing region of rats, 8 kHz near the most sensitive region of normal rat audiogram
181 (Parthasarathy et al. 2014) and hearing of frequencies higher than 8 kHz being most
182 vulnerable to blast injury (Race et al. 2017). The sound levels of clicks and pips
183 ranged from 90 to 10 dB peak SPL in 5-dB steps. All stimuli were presented in
184 alternating polarity at 26.6 per second with 1500 repetitions (750 at each polarity). A
185 20 msec acquisition window (0-20 msec) was used.

186 Data were processed with a 30 Hz high-pass (HP) filter and a 3000 Hz low-pass (LP)
187 filter prior to analysis. The ABR threshold was visually determined as the minimum
188 sound level that produced a distinct ABR waveform, with confirmation from two other
189 researchers. The ABR amplitudes of waves I and V from channel 2 were estimated

190 as the differences of each wave's amplitude, as seen in BioSigRP (TDT) and the
191 baseline amplitude (measured as an average of 2 msec waveform prior to the
192 cochlear microphonic).

193

194 6 Sham animals and 8 Blast animals were used in MLR analysis. For MLR, similar
195 rectangular clicks and 8 kHz tone pips of alternating polarity as in ABR were used
196 but were presented at a slower rate (3.33/sec vs. 26.6/sec in ABRs) and with a
197 recording window of longer duration (100 msec vs. 20 msec in ABRs). This time
198 window provides enough time to capture the stimulus-evoked "middle-latency"
199 neural responses from the auditory midbrain, thalamus and cortex (Barth and Shi Di
200 1991; McGee et al. 1991; Di and Barth 1992; McGee and Kraus 1996; Phillips et al.
201 2011; Šuta et al. 2011) alongside ABR. Stimuli were presented at 80 dB sound
202 pressure level (SPL) and 30 dB sensation level (SL, 30 dB above corresponding
203 ABR thresholds), as determined in the previous ABR recordings. 1500 repetitions
204 were collected over an acquisition time window of 100 msec to obtain an average
205 response. Only one animal exhibited hearing threshold higher than 80 dB SPL at
206 only one time point, for which MLR recording has been excluded for that point.

207 Channel 2 was used for MLR analyses, and results were qualitatively similar for
208 channel 1. Data were processed with HP (fc = 10 Hz) and LP (fc = 300 Hz) filters
209 prior to analysis.

210

211 **EFRs**

212 EFRs were recorded during the same recording session following ABRs and MLRs
 213 using the same electrode configurations with similar techniques to Lai and Bartlett
 214 (2018) and Lai (Lai et al. 2017). The two channels were sensitive to a
 215 complementary range of amplitude modulation frequencies (AMFs) (Parthasarathy
 216 and Bartlett 2012), with channel 1 (mid-sagittal) being more sensitive to higher AMFs
 217 (90-2048 Hz) while channel 2 (interaural) is more sensitive to lower AMFs (8-90 Hz).
 218 The AM stimuli used for EFRs were sinusoidally amplitude-modulated (AM) sounds,
 219 with Gaussian noise, 8 kHz tone, or 16 kHz tone as carriers, and under 100% and 50%
 220 modulation depth with a stimulus duration of 200 msec. The AMFs selected for this
 221 study are 10 Hz, 45 Hz, and 256 Hz, based on the findings in Race et al. (Race et al.
 222 2017), which found significant differences, particularly at the lower AMFs. The
 223 acquisition window was 300 msec long, and each response was an average of 200
 224 repetitions. The stimuli were presented at 30 dB SL. For animals that had a hearing
 225 threshold above 70 dB SPL, which usually happens on day 1 post-exposure, EFR
 226 was not collected at the time point due to the limitation of the speaker and BiosigRP.
 227
 228 For AM in Noise stimuli, the same EFRs were used alongside a 71 Hz sinusoidally
 229 AM masker of the same length and onset, with Gaussian noise as the carrier, similar
 230 to Lai and Bartlett (Lai and Bartlett 2018). Noise AM maskers were presented at
 231 sound levels of 20dB SNR and 0SNR to the sound level of target AM. Prior to EFR
 232 amplitude analysis, data were passed through an LP filter of 3000 Hz and a
 233 high-pass filter that was either slightly below the AMF for AMFs <90 Hz, or 80 Hz for

234 AMFs ≥ 90 Hz.

235

236 **IRNs**

237 For 6 Sham animals and 8 Blast animals, IRNs were recorded during the same
238 recording session following the previous stimuli using the same electrode
239 configurations. The sound level of presentation was 30 dB SL (above click hearing
240 threshold). Data for animals with a hearing threshold above 70 dB SPL were not
241 collected at the time point.

242

243 IRN tone stimuli were created by sequential delay and add operations. Time-varying
244 pitch curves were created by applying polynomial equations to create delays
245 constructed from the fundamental frequencies of Chinese tone 2 and tone 4,
246 delaying Gaussian noise (80 Hz-40 kHz) by the inversion of pitch and adding it back
247 on itself in a recursive manner (Yost 1996a). The core MATLAB program used for
248 generating IRN was modified from Krishnan et al. (Krishnan et al. 2014, 2015) This
249 would generate dynamic, curvilinear pitch patterns (Swaminathan et al. 2008) that
250 preserves variations in pitch using a broadband carrier. The number of iteration
251 steps for these stimuli was 32, beyond which there is little or no change in pitch
252 salience (Yost 1996b).

253

254 IRN iteration (ite) stimuli were created with the same polynomial equations used for
255 tone 2, but with different iterations to create an array of IRN stimuli with different pitch

256 salience. The numbers of iteration steps were 32, 16, 8, 4, and 2.

257 All IRN stimuli consisted of pairs of waveforms in original and inversed polarities to

258 compensate for envelope or fine structure response under different calculations and

259 cancel any microphonics. The stimulus duration was 250 msec, and the acquisition

260 window was 300 msec long. Each response was an average of 200 repetitions.

261 Given the main frequencies involved in the IRN autocorrelation (>100 Hz), channel 1

262 was used for IRN analyses, and results were qualitatively similar for channel 2.

263

264 **Statistics**

265 Statistics were performed with statistics software JASP (Version 0.11, JASP Team,

266 2019). All statistics for ABR and EFR utilized 2-way repeated measures ANOVA test

267 ($\alpha = 0.05$) to check the significance of each main effect and interaction, undergoing

268 Greenhouse-Geisser sphericity corrections (Greenhouse and Geisser 1959) and

269 Tukey Post Hoc corrections (Tukey 1949). For ABR statistics, Wave I (channel 2), III

270 (channel 1) and V (channel 2) were measured at each time point (Fig. 1B),

271 corresponding to the auditory nerve (Wave I), cochlear nucleus (Wave III), and

272 rostral brainstem/IC sources (Wave V) (Parthasarathy and Bartlett 2012; Simpson

273 and Prendergast 2013). For EFR statistics, responses were analyzed from channel 2

274 for 10 Hz and 45 Hz, and from channel 1 for 256 Hz (Parthasarathy and Bartlett

275 2012). Prior to statistical tests, EFR amplitudes at signal frequencies were acquired

276 through Fast Fourier Transformation (FFT) in MATLAB (MathWorks) similar to (Lai

277 and Bartlett 2018).

278

279 For MLR statistics, P1, N1, P2, and N2 (Fig. 5A) peaks were measured at each time
280 point, corresponding to subcortical (P1), thalamocortical (N1) and cortical sources
281 (P2, N2) (Simpson and Prendergast 2013). Peak amplitudes were normalized to the
282 pre-blast exposure baseline measurements for display in Fig. 5C, D. The normalized
283 peak amplitudes at each time point were compared to the pre-stimulus baseline
284 using a paired sign-rank test, with a 0.05 significance criterion.

285

286 For IRN statistics, we performed moving-window autocorrelations in 25 msec moving
287 windows (5 msec steps) on each response waveform to simulate physiological
288 tracking of temporal periodicity. Peak autocorrelation frequency was defined by the
289 inverse of the time lag where peak autocorrelation value occurs in each window. This
290 process yielded a peak frequency that reflect the frequency representation of the
291 IRN auditory response for each of the 51 time windows in total (see Fig. 8B). Of
292 those, 45 occurred during the stimulus. The peak frequencies were then compared
293 to the “pseudopitches” of the IRN stimuli on corresponding time points. A value within
294 5 Hz of absolute difference to corresponding “pseudopitch” was considered “tracked.”
295 We used this number of “tracked” peak frequencies, or “pitch-tracking score,” as a
296 quantification for IRN performance. The significance of each main effect (time, blast
297 condition, and IRN iterations) and interaction was assessed using similar 2-way
298 repeated measures ANOVA test as ABR statistics ($\alpha = 0.05$). For
299 response-to-response correlation (Fig. 8D), the cross-correlation was measured

300 between the response to the IRN stimuli pre-exposure and the response to the same
301 stimulus post-exposure. Blast versus sham group was tested using the paired
302 sign-rank test for this measure ($\alpha = 0.05$).

303

304 **Results**

305 **A. ABR and MLR**

306 **ABR Thresholds**

307 *(Insert Fig. 2 about here)*

308 Click ABR recordings captured distinctive courses of threshold changes over the two
309 months post-exposure for blast and sham animals (Fig. 2). A large, >30dB SPL
310 maximum threshold increase was observed in post-blast-exposure animals (Fig. 2,
311 red lines). Adjacent animals exposed only to blast noise (Sham) did not undergo
312 significant threshold shifts (Fig. 2, blue lines). Thresholds for blast group animals
313 showed clear recovery during the first two weeks, with the largest changes occurring
314 between 4 days – 10 days. Thresholds for blast-exposed animals remained
315 significantly elevated (worse) than those of sham animals throughout the two months
316 post-exposure that were measured (Simple Main Effects, day 30: $df=1.000$,
317 $F=10.904$, $p=0.005$; day 60: $df=1.000$, $F=12.727$, $p=0.003$). Significant main effects
318 of both Group ($df=1.000$, $F=61.943$, $p<0.001$, $\eta^2_p=0.816$) and Time Point ($df=2.554$,
319 $F=41.932$, $p<0.001$, $\eta^2_p=0.750$), as well as a significant Group*Time Point interaction
320 effect ($df=2.554$, $F=23.503$, $p<0.001$, $\eta^2_p=0.627$), were observed.

321

322 Similar trends were observed with tone ABR recordings of 8 kHz and 16 kHz (Fig. 2),
 323 with a significant ($p \leq 0.001$) >30 dB increase in threshold within 48 hours
 324 post-blast-exposure and most prominent recovery between 4 days – 10 days. 8 kHz
 325 threshold differences between blast conditions became non-significant ((Simple
 326 Main Effects, $df=1.000$, $F=3.151$, $p=0.098$) at 10 days post-blast. At two weeks
 327 post-exposure, 16 kHz thresholds remained significantly elevated (Simple Main
 328 Effects, $df=1.000$, $F=16.527$, $p<0.001$), after which point the thresholds for the two
 329 chosen tone frequencies were no longer significantly different between Blast and
 330 Sham. Our rmANOVA analysis using Group and Time Points as factors showed
 331 significant main effects of Group (8 kHz: $df=1.000$, $F=10.847$, $p=0.005$, $\eta^2_p=0.437$; 16
 332 kHz: $df=1.000$, $F=19.697$, $p<0.001$, $\eta^2_p=0.585$), Time (8 kHz: $df=3.924$, $F=25.837$,
 333 $p<0.001$, $\eta^2_p=0.649$; 16 kHz: $df=3.043$, $F=20.181$, $p<0.001$, $\eta^2_p=0.590$) and
 334 Group*Time Point interaction (8 kHz: $df=3.924$, $F=13.490$, $p<0.001$, $\eta^2_p=0.491$; 16
 335 kHz: $df=3.043$, $F=15.860$, $p<0.001$, $\eta^2_p=0.531$) for 8 kHz and 16 kHz threshold
 336 respectively. These results demonstrate that broadband click thresholds remain
 337 significantly elevated over the 60 days measurement window. 8 kHz thresholds
 338 largely returned to baseline (Day 30: 8 dB difference, $t=3.197$, $p=0.118$; day 60: 4 dB
 339 difference, $t=1.598$, $p=0.965$) after two weeks, and 16 kHz thresholds remained
 340 significantly elevated compared to pre-blast baseline according to post hoc analysis
 341 (Day 30: 15.5 dB difference, $t=5.687$, $p<0.001$; day 60: 14.5 dB difference, $t=5.320$,
 342 $p<0.001$), although the difference between blast and Sham was not significant at

343 these time points.

344

345 **ABR Amplitudes**

346 *(Insert Fig. 3 about here)*

347 For our ABR and MLR measurements, we used two sound levels: 80 dB SPL was
 348 chosen because it is commonly used in auditory evoked potential studies in rat and
 349 human studies (Simpson et al. 1985; Alvarado et al. 2012; Race et al. 2017), and it
 350 elicits clear ABR responses in all except the most extreme cases of blast-exposure.
 351 In order to compensate for changes in threshold induced by blast exposure, we also
 352 measured ABR amplitudes at 30 dB SL above threshold (sensation level, or SL).
 353 This enabled us to separate changes in ABR amplitudes due to audibility (threshold)
 354 versus those due to threshold-independent changes in subcortical auditory signaling.
 355 Note that we did not attempt to compare later ABR waves with equivalent wave I
 356 amplitudes, as in Lai et al. (2017).

357

358 ABR wave amplitudes were assessed for wave I (putative auditory nerve), III
 359 (putative cochlear nuclei), and V (putative rostral brainstem and inferior colliculus) in
 360 response to click stimuli at 80 dB SPL (Fig. 3) and 30 dB SL (Fig. 4). Repeated
 361 measures statistics for 80 dB SPL and 30dB SL are shown in Tables 1-4.

362 **Wave I:** Wave I amplitudes at 80 dB SPL for all ABR carriers at 80 dB SPL exhibited
 363 significant main effects of Group, Time, and Group*Time interaction (Table 1).

364 Compared to pre-exposure responses, wave I amplitudes were significantly smaller

at all time points tested in blast animals for clicks, 8 kHz tones, and 16 kHz tones, indicating lasting cochlear/auditory nerve damage (Table 4). No significant changes in wave I amplitudes were observed in Sham exposed animals at any time point.

Wave III: Wave III amplitudes at 80 dB SPL for all ABR carriers at 80 dB SPL exhibited significant main effects of Group, Time, and Group*Time interaction (Table 1), with Group effects lasting for 14 days for Click and 16 kHz tones and 10 days for 8 kHz tones. Compared to pre-exposure responses, wave III amplitudes were significantly smaller at all time points tested in blast animals for clicks and 16 kHz tones and up to 30 days for 8 kHz tones, indicating lasting declines in cochlear nucleus excitation (Table 4). No significant changes in wave III amplitudes were observed in Sham exposed animals at any time point.

Wave V: Wave V amplitudes at 80 dB SPL for all ABR carriers at 80 dB SPL exhibited significant main effects of Group, Time, and Group*Time interaction (Table 1), with Group effects lasting for 14 days for Click and 16 kHz tones and 7 days for 8 kHz tones. Compared to pre-exposure responses, wave V amplitudes were significantly smaller at all time points tested in blast animals for clicks, indicating lasting declines in rostral brainstem/IC excitation for brief, broadband clicks (Table 4). However, decreases in wave V amplitudes persisted for only 7 days for 8 kHz tones and 14 days for 16 kHz tones, suggesting that despite decreases in cochlear nucleus excitation (as represented by wave III amplitude), rostral brainstem/IC responses compensated and restored their responses. No significant changes in wave V amplitudes were observed in Sham exposed animals at any time point except for a

387 small decline for 16 kHz responses 60 days post Sham exposure (Table 4).

388

389 ***(Insert Fig. 4 about here)***

390

391 The effects on ABR waves were greatly diminished when responses to 30 dB SL
392 sounds were measured, as shown in Table 2 and Table 3. For Wave I, significant
393 main effects of Time (Click: $df=4.360$, $F=2.554$, $p=0.043$, $\eta^2_p=0.154$; 8 kHz: $df=4.264$,
394 $F=3.146$, $p=0.018$, $\eta^2_p=0.183$; 16kHz: $df=4.469$, $F=2.325$, $p=0.031$, $\eta^2_p=0.142$) but
395 not Group (Click: $df=1.000$, $F=3.637$, $p=0.077$, $\eta^2_p=0.206$; 8 kHz: $df=1.000$, $F<0.001$,
396 $p=0.994$, $\eta^2_p<0.001$; 16kHz: $df=1.000$, $F=1.046$, $p=0.324$, $\eta^2_p=0.070$) were observed
397 for click, 8 kHz, and 16 kHz. Additionally, significant Group*Time interaction effects
398 were only observed for Click ($df=4.360$, $F=2.630$, $p=0.039$, $\eta^2_p=0.158$) and 16 kHz
399 ($df=4.469$, $F=2.381$, $p=0.027$, $\eta^2_p=0.145$). Simple main effects of Group ($df=1.000$)
400 were only observed in Click (Table 3).

401 Compared to pre-exposure responses, wave I and V responses to clicks were
402 significantly reduced 1 day post-blast and wave III responses were significantly
403 reduced days 1-4. Otherwise, there were no significant declines in wave amplitudes
404 in the Blast group, and there were no significant amplitude changes in the Sham
405 group.

406

407 ***(Insert Fig. 5 about here)***

408

409 B. MLR

410 In order to observe thalamocortical and cortical neural transmission in response to
 411 acoustic transients, we recorded middle-latency auditory responses to click and 8
 412 kHz tone stimuli. These stimuli were identical to those used for ABR, but the
 413 presentation rate was much slower, and the analysis window and filters were
 414 different (see Methods). Measurements were made for the first four main peaks of
 415 the MLR. Here, P1 corresponds to subcortical activity, largely encompassing the
 416 ABR. N1 corresponds to thalamocortical transmission, while P2 and N2 are thought
 417 to correspond to primarily cortical activity (Deiber et al. 1988; Liégeois-Chauvel et al.
 418 1994; Tichko and Skoe 2017; Musiek and Nagle 2018).

419

420 80 dB SPL responses

421 In blast animals, all waves were decreased relative to pre-blast baseline for days 1-7
 422 post-blast ($p < 0.05$, sign-rank test) in response to 80 dB SPL click stimuli. Simple Main
 423 effect of blast showed similar results for P1, N1 and P2 (Table 5). Grand average
 424 traces are shown for MLR responses in this time window in Fig. 5A, relative to the
 425 pre-blast waveform (thick blue line in A-D). Even after the blast, the morphology and
 426 timing of the MLR waveform remained relatively intact, but the amplitudes were
 427 significantly diminished, shown as a significant Time*Group interaction effect for all
 428 three waves of interest (P1: $df=2.942$, $F=4.111$, $p=0.014$, $\eta^2_p=0.255$; N1: $df=3.460$,
 429 $F=7.786$, $p < 0.001$, $\eta^2_p=0.393$; P2: $df=3.684$, $F=5.607$, $p=0.001$, $\eta^2_p=0.318$). In Fig.
 430 5E-H, wave amplitudes were normalized to the pre-blast waves and measured.

431 Between 7 and 10 days, the early P1 wave recovers to within 10-15% of its baseline
432 amplitude, whereas the later waves recovered more slowly (Fig. 5E). In particular, the
433 N1 wave, thought to reflect thalamocortical transmission (Barth and Shi Di 1991;
434 McGee et al. 1991, 1992; Di and Barth 1992; Brett et al. 1996; McGee and Kraus
435 1996; Phillips et al. 2011; Šuta et al. 2011), remained significantly lower in blast
436 animals even 60 days post-blast ($p < 0.05$, sign-rank test, Fig. 5E). By contrast, the
437 MLR waves in sham animals were largely stable across the measurement time (Fig.
438 5F). Although there was some decline in the later waves for the last time window, this
439 was not statistically significant (Fig. 5B, D, F).

440

441 MLR responses to 8 kHz, 80 dB SPL tone pips largely mirrored the results to clicks,
442 with significant decreases for all waves for post-blast days 1-7 and a lasting decline
443 in N1 for the duration of measurements ($p < 0.05$, sign-rank test, traces not shown).
444 Sham responses did not show any significant changes in MLR waves in response to
445 the 80 dB SPL tone pips.

446

447 **30 dB SL**

448 MLR responses to clicks at 30 dB SL were reduced in Blast animals 1 day after the
449 blast but recovered to baseline levels afterwards. There was a tendency towards
450 elevated P1 amplitudes, but this was not significant (Fig. 5G). Sham animals did not
451 show any significant changes, though there was a tendency towards an increase in
452 wave amplitude (Fig. 5H). Similar results were found for responses to tones at 30 dB

453 SL (not shown).

454

455 **C. EFR and EFR in noise**

456 Given the different time courses and extents of ABR threshold change for clicks and
 457 tones, we measured the corresponding EFRs in response to Gaussian broadband
 458 noise (nSAM), 8 kHz, and 16 kHz sinusoidal tone carriers. Considering that slow AM
 459 (<50 Hz) and faster AM (>50 Hz) are differentially represented throughout cortical
 460 and subcortical auditory nuclei (Joris et al. 2004; Wang et al. 2008), three
 461 representative AMFs (10, 45, and 256 Hz) were selected from previous publications
 462 (Parthasarathy et al. 2010, 2014; Parthasarathy and Bartlett 2011, 2012; Race et al.
 463 2017) and tested in quiet at 100% and 50% modulation depth. AM stimuli were also
 464 presented at 30 dB SL with a 71 Hz sinusoidally AM masker of the same length and
 465 onset, with Gaussian noise as the carrier, at 20dB SNR and 0 SNR relative to the
 466 sound level of target AM. Responses were collected from both electrodes, but for 10
 467 and 45 Hz AMFs, channel 2 responses were analyzed; and for 256 Hz AMF, channel
 468 1 responses were analyzed (see Methods). For each carrier, simple main effects of
 469 all conditions were analyzed.

470 ***(Insert Fig. 6 about here)***

471

472 **EFRs in quiet:** For all three carriers in quiet, EFR amplitudes were similar at 10 and
 473 256 Hz across time points and AM modulation depths (Fig. 6). Overall, the nSAM
 474 FFT amplitudes were higher in the Blast group in quiet (df=5.000, F=9.629, p=0.008,

475 $\eta^2_p=0.426$), with 45 Hz being the most affected. Interestingly, in contrast to the lower
 476 FFT Amplitude found in Blast AM at 80 dB SPL (Race et al. 2017), when 30 dB
 477 sensation level (threshold +30 dB) was to compensate for threshold differences, FFT
 478 amplitude of 45 Hz nSAM was higher in Blast than in Sham animals (Fig. 6B). This
 479 difference was most salient on day 7 for 45 Hz nSAM (Post hoc comparison:
 480 $t=-4.122$, $p=0.006$). For 8 kHz SAM and 16 kHz SAM, the slight elevation of AM FFT
 481 Amplitude in Blast animals was not significant (Fig. 6C and 6D). Surprisingly, time
 482 did not have a significant interaction across repeated measures for AM response
 483 with any carrier either.

484

485 **EFR in noise:** Not surprisingly, Noise level and Modulation Depth both had a
 486 significant repeated measures effect on nSAM (Noise level: $df=2.000$, $F=263.217$,
 487 $p<0.001$, $\eta^2_p=0.953$; Depth: $df=1.000$, $F=455.655$, $p<0.001$, $\eta^2_p=0.972$), 8 kHz SAM
 488 (Noise level: $df=2.000$, $F=19.308$, $p<0.001$, $\eta^2_p=0.580$; Depth: $df=1.000$, $F=72.031$,
 489 $p<0.001$, $\eta^2_p=0.837$) and 16 kHz SAM (Noise level: $df=2.000$, $F=16.691$, $p<0.001$,
 490 $\eta^2_p=0.544$; Depth: $df=1.000$, $F=49.742$, $p<0.001$, $\eta^2_p=0.780$). Noise level and Depth
 491 also have a significant interaction effect with Groups for nSAM overall (Noise level:
 492 $df=2.000$, $F=10.295$, $p<0.001$, $\eta^2_p=0.442$; Depth: $df=1.000$, $F=6.057$, $p=0.029$,
 493 $\eta^2_p=0.318$), showing blast nSAM responses as less affected 20 SNR noise, but more
 494 sensitive to AM attenuation for lower modulation depth (Fig. 7B). Noise level also
 495 affect sham animals less than blast animals for 8 kHz SAM overall, showing a
 496 significant interaction effect with Group ($df=2.000$, $F=5.696$, $p=0.008$, $\eta^2_p=0.289$, Fig.

7C). These conditions do not have significant interaction effects with Group on 16 kHz SAM (data not shown). Noise level had significant interaction effects with both Group ($df=2.000$, $F=6.130$, $p=0.011$, $\eta^2_p=0.320$) and Depth ($df=2.000$, $F=19.438$, $p<0.001$, $\eta^2_p=0.599$) for nSAM 45 Hz, while the effect of Time or Depth between Groups is not significantly different for any modulation frequency.

502

(Insert Fig. 7 about here)

504

For 8 kHz SAM, the effects of Noise level were applied differently between Groups, as significant interaction effects were observed between Noise and Group for 10 Hz ($df=2.000$, $F=12.795$, $p=0.001$, $\eta^2_p=0.477$) and 45 Hz ($df=2.000$, $F=4.878$, $p=0.015$, $\eta^2_p=0.258$) modulation frequencies, though not for 256 Hz (data not shown). Most notably, sham 8 kHz SAM EFRs showed greater resilience to competing noise at 10 Hz modulation frequency (Fig. 7C), contrary to the trends observed in nSAM. Modulation Depth affects FFT amplitude without regard to blast condition, with no significant interaction effects with Group observed. For 16 kHz SAM, none of the parameters tested had significantly different effects between Groups at 30 dB SL (not shown).

515

Overall, Blast and Sham animals generally decreased EFR amplitudes with increased noise, especially for 0 dB SNR. Similar to quiet, 45 Hz amplitudes were most affected, with increases in EFR amplitudes in Blast animals that were most

519 pronounced in the 7-14 day window (Fig. 7B). The effects and interactions of blast
520 exposure and competing noise were dependent on both modulation frequency and
521 time after exposure..

522

523 **D. IRN**

524 Time-varying IRN stimuli (Fig. 8A) were used to elicit frequency-following response
525 (FFR) mimicking Mandarin tone 2 (T2, rising) and tone 4 (T4, falling) pitch contours
526 to measure pitch-tracking ability using a broadband speech-like carrier at 30 dB SL,
527 similar to what has been measured in human studies of auditory learning and
528 hearing loss (Anderson et al. 2010, 2013; Skoe and Kraus 2010). We used
529 autocorrelation interval contours that simulated pitches similar to the forms of rising
530 (T2) and falling (T4) pitch contours of the Mandarin Chinese vowel /yi/ (Krishnan et al.
531 2014, 2015, 2017a, 2017b). IRN responses collected from channel 1 were evaluated
532 based on the pitch-tracking score (Fig. 8B), which measures the number of time
533 windows where the dominant autocorrelation frequency of the response matches
534 that of the IRN stimulus autocorrelation frequency (see Methods). In general, we
535 observed a loss of pitch-tracking fidelity in Blast animals over the two months
536 post-exposure (Fig. 8B and 8C). Even for the most salient pitch (32 iterations), blast
537 exposure had a significant Group effect on pitch-tracking scores in both Tone 2
538 ($df=1.000$, $F=6.495$, $p=0.026$, $\eta^2_p=0.351$) and Tone 4 ($df=1.000$, $F=6.115$, $p=0.029$,
539 $\eta^2_p=0.338$), with the largest mean differences on day 7-10. The interaction effect
540 between Time and Group was not significant.

541 Blast exposure significantly changed the neural response's morphology to IRN at 30
542 dB SL ($p=0.016$, paired sign-rank test, Fig. 8D), such that the cross-correlation
543 between the pre-exposure response and the post-exposure response was much
544 lower in the Blast group up to 30 days post-blast.

545 ***(Insert Fig. 8 about here)***

546

547 **IRN iterations:** As expected, reduced pitch salience, controlled by reducing iteration
548 number, affected pitch-tracking responses in animals ($df=4.000$, $F=41.697$, $p<0.001$,
549 $\eta^2_p=0.777$), also showing a significant interaction effect with Time post-exposure
550 ($df=20.000$, $F=1.722$, $p=0.031$, $\eta^2_p=0.125$). Specifically, pitch-tracking performances
551 to 32 iterations and 16 iterations worsened significantly up to 7-10 days
552 post-exposure, with various degrees of recovery over the following time course. Both
553 the Blast and Sham group exhibited worse pitch tracking with reduced iterations
554 (salience) and to a similar degree. No significant interaction effects with Group were
555 observed for Time and Iterations (Fig 9).

556 ***(Insert Fig. 9 about here)***

557

558 **Discussion**

559 This study examined the time course of recovery from a single mild blast injury using
560 simple and complex auditory stimuli longitudinally at dense time points for two
561 months. The largest blast-induced threshold shifts and changes in evoked potentials
562 diminished within two weeks. At 30-60 days post-blast, lingering increases in click

(but not tone) thresholds, decreases in MLR N1 (thalamocortical) amplitude, and declines in pitch-tracking of speech-like IRN pitch trajectories were observed. Compensating for threshold shift and using 30 dB sensation level for AM stimuli, we found that responses to sinusoidal AM stimuli in quiet or noise recovered within 14 days. The 7-14 day window was particularly rapid in the recovery of many auditory parameters.

Lasting changes from a single mild blast

This study has examined injuries elicited by a single dorsal blast exposure with body shielding that did not result in tympanic membrane ruptures, which we and others characterize as a “mild” blast exposure. Therefore, the deficits observed may not be as drastic as that documented by some previous studies in which the injuries were caused by more intense or multiple exposures (Cho et al. 2013b; Du et al. 2013; Luo et al. 2014a, 2014b; Mahmood et al. 2014), often resulting in death or tympanic membrane rupture. The distribution of injuries also differed from models in which blast exposure comes from different orientations, as predicted in animals (Chavko et al. 2011; Dal Cengio Leonardi et al. 2012) and computational studies (Hua et al. 2017; Unnikrishnan et al. 2019). These differences in pressure wave amplitude, duration, and propagation patterns would affect both the distribution and severity of damage across the brain. Compared to other orientations, including top-facing exposure as in our model, head-facing exposure is known to produce the highest peak pressure and prolonged pressure wave propagation, while side-facing

585 exposure produced lower peak pressure and pressure increase rate in rat model
586 (Chavko et al. 2011; Dal Cengio Leonardi et al. 2012). Although these could change
587 the potential mechanisms of recovery and compensation, it is likely that all blast
588 exposures undergo a multi-stage recovery process similar to that observed in the
589 present study. In our model, the overpressure blast wave passes through the entire
590 rat brain, such that TBI can be observed throughout the brain, including the frontal
591 cortex and in multiple thalamic regions (Walls et al. 2016), and it results in increased
592 ventral BBB membrane permeation and inflammation, encompassing many
593 subcortical auditory nuclei and axonal tracts. The non-invasive physiological
594 measurements in this study may be indicators of more widespread blast damage in
595 auditory and may be correlated with damage in non-auditory brain regions.

596

597 **ABR**

598 We documented a >30 dB peak increase in threshold for click, 8 kHz, and 16 kHz
599 (Fig. 2) during the first 4 days, consistent with the description of IHC and OHC
600 disturbances across a wide range of frequencies due to blast overpressure as stated
601 in multiple previous publications (Patterson and Hamernik 1997; Ewert et al. 2012;
602 Race et al. 2017). Although this broadband threshold shift extended to the last time
603 point at 60 days, the ~10 dB difference would not be considered clinically relevant
604 and suggests .

605 Rapid improvements in ABR threshold and wave amplitudes were observed in the
606 7-10 days recovery period for waves I, wave III, and wave V (Fig. 3). Notably, wave V

607 amplitude recovered earlier than wave I, possibly indicating the role of compensation
608 in auditory midbrain as one of the post-blast recovery mechanisms.

609

610 ABR parameters showed two waves of post-blast changes: one between 1-10 days
611 post-exposure, and one 10-30 days, as evidenced by Figs. 2 and 3. We hypothesize
612 that these two waves of deficits indicated a series of secondary biochemical impacts
613 surrounding CAS (Laplaca et al. 1997; Knudsen and Øen 2003; Hamann et al. 2008;
614 Garman et al. 2011; Säljö et al. 2011; Luo et al. 2014a, 2014b; Song et al. 2015;
615 Walls et al. 2016). In the initial recovery window, we observed changes in ABR
616 waveforms over and above those expected by threshold shifts, whereas for days 10
617 and afterwards, there were changes observed at 80 dB SPL but not for 30 dB SL.
618 Our observations of blast recovery were mostly consistent with the notion of changes
619 over the first week due to secondary damage that is substantially repaired over the
620 second week.

621

622 **MLR**

623 At 80 dB SPL, we found persistent deficits in thalamocortical and cortical
624 transmission based on the N1, P2 and N2 peaks (Fig. 5A vs. B, C vs. D), which were
625 affected at 30 and 60 days, even after the early P1 response had fully recovered (Fig
626 5E). These deficits were not present at 30 dB SL, suggesting that effects were at
627 least partially due to small shifts in auditory thresholds (Fig. 5G). In veterans and the
628 general population with lifetime noise exposure, MLR responses were shown to be

629 smaller even when subjects had clinically normal audiograms, and there was some
630 evidence of increased cortical gain (Valderrama et al. 2018; Bramhall et al. 2020). In
631 another study with blast-exposed veterans, most of the changes in auditory-evoked
632 potentials were correlated with hearing loss (Meehan et al. 2019). Together, these
633 results suggest that hearing loss may be the main contributor to MLR changes
634 leading to declines in suprathreshold responses.

635

636 **Amplitude Modulation EFRs**

637 The current study extended an earlier study (Race et al. 2017) to include EFR
638 responses to more challenging auditory stimuli, including lower modulation depth
639 (Fig 6) and in the presence of modulated noise (Fig 7). The Race et al. (Race et al.
640 2017) study revealed differences in AM processing at 80 dB SPL between Blast and
641 Sham animals, such that blast animals had lower AM FFR amplitudes mainly for AM
642 frequencies ≤ 50 Hz. However, when the hearing threshold has been compensated,
643 the differences in AM FFR amplitude diminished and even changed sign (Fig. 6),
644 suggesting that both changes in audibility and changes in the gain of subcortical
645 auditory system are critical contributors to AM FFR deficits in the blast-exposed
646 auditory system. There are complicated interactions between the AM FFR
647 amplitudes, blast exposure, and the presence of noise, evident as a persistent
648 Group*Noise Level interaction effect in both nSAM and 8 kHz SAM. AM responses
649 consist of contributions from multiple generators along the auditory neuraxis, with
650 cortical generators contributing mainly to lower AMFs <50 Hz, and higher frequency

651 AM responses limited to nuclei lower in the auditory neuraxis. The lack of
652 blast-induced differences at higher AMFs distinguishes the blast-induced damage
653 from age-related changes, which are most prominent at higher modulation
654 frequencies (Parthasarathy et al. 2010, Parthasarathy and Bartlett 2012, Lai et al.
655 2017).

656

657 The differences in low-middle AMFs were manifested in opposed directions under
658 slow (10 Hz) and middle (45 Hz) AMFs: notably, repeated measures testing showed
659 that FFT amplitudes of 8 kHz SAM in noise are lower for Blast at 10 Hz modulation
660 frequency (Day 4 quiet, 100% depth: Blast mean=0.496 mV, Sham mean=0.704 mV),
661 but higher for Blast at 45 Hz (Day 4 quiet, 100% depth: Blast mean=0.898 mV, Sham
662 mean=0.733 mV ; Fig 7C). This dichotomy is ripe for further study since the 10 Hz
663 and 45 Hz modulations represent different temporal processing regimes and
664 components of speech (Rosen 1992). If these modulation frequency bands are
665 differentially altered by blast, it may skew the cochlear-filtered envelope and impair
666 hearing in complex listening environments (Chabot-Leclerc et al. 2016).

667

668 **IRN EFRs**

669 Complex temporal periodicity between 50 Hz and 500 Hz carries important speech
670 information such as voicing, stress and intonation (Rosen 1992). The present study
671 provided insights into blast-induced sound processing deficits through the use of an
672 IRN stimulus that simulates Chinese intonations and whose pitch and salience can

673 be reliably controlled, showing that IRN can be a useful diagnostic tool for
674 neurotrauma. We found that even when click ABR thresholds have returned to
675 subclinical threshold shifts, the deficits in pitch-tracking response to IRN tone stimuli,
676 lingered at least 30 days post-exposure (Figs. 8D).

677 Both Blast and Sham animals showed an overall reduction in tracking with
678 decreased salience through decreased iterations in IRN, but differential effects were
679 noted mainly only in the first two weeks. A previous study showed that increased IRN
680 iterations improved auditory stream segregation in normal hearing veterans more
681 than hearing-impaired veterans (Thompson and Marozeau 2014). Our IRN data
682 (Figs. 8-9) suggest that more dynamic and speech-like modulation changes do not
683 recover quickly or completely from even a single mild blast exposure.

684

685 **Acknowledgments**

686 The authors would like to thank Jonathan Tang, Brandon Coventry, Alex Sommers,
687 Nanami Miyazaki, and all the other members in Central Auditory Processing Lab and
688 Lab of Translational Neuroscience for their generous assistance in the completion of
689 this study.

690

691 **Author contributions**

692 Study concept and design: Edward Bartlett, Riya Shi, Emily X. Han, Joseph M.
693 Fernandez.
694 Animal Blast Exposure: Joseph M. Fernandez.

695 Electrophysiology: Emily X. Han, Caitlin Swanberg.

696 Data analysis and interpretation: Emily X. Han, Edward Bartlett, Joseph M.

697 Fernandez.

698 Writing of the manuscript: Emily X. Han, Edward Bartlett.

699 Critical revision of the manuscript: Riya Shi, Joseph M. Fernandez, Caitlin Swanberg.

700 Study supervision and obtainment of funding: Edward Bartlett, Riya Shi.

701

702 **Funding**

703 This study is funded by Indiana CTSI 11917 and NIH T32DC016853.

704

705 **Disclosures**

706 Riya Shi is a co-founder of Neuro Vigor, a company developing novel drug treatments

707 and diagnostic approaches for neurodegenerative diseases and neurotrauma.

708

709 **References**

- 710 **Alsindi S, Patterson RD, Sayles M, Winter IM.** The responses of single units to
711 simple and complex sounds from the superior olivary complex of the Guinea pig. In:
712 *Acta Acustica united with Acustica*. S. Hirzel Verlag GmbH, 2018, p. 856–859.
- 713 **Alvarado JC, Fuentes-Santamaría V, Jareño-Flores T, Blanco JL, Juiz JM.**
714 Normal variations in the morphology of auditory brainstem response (ABR)
715 waveforms: A study in wistar rats. *Neurosci Res* 73: 302–311, 2012.
- 716 **Anderson S, Parbery-Clark A, White-Schwoch T, Kraus N.** Auditory brainstem
717 response to complex sounds predicts self-reported speech-in-noise performance. *J*
718 *Speech, Lang Hear Res* 56: 31–43, 2013.
- 719 **Anderson S, Skoe E, Chandrasekaran B, Kraus N.** Neural timing is linked to
720 speech perception in noise. *J Neurosci* 30: 4922–4926, 2010.
- 721 **Barth DS, Shi Di.** The functional anatomy of middle latency auditory evoked
722 potentials. *Brain Res* 565: 109–115, 1991.
- 723 **Bendor D, Wang X.** The neuronal representation of pitch in primate auditory cortex.
724 *Nature* 436: 1161–1165, 2005.
- 725 **Berger G, Finkelstein Y, Avraham S, Himmelfarb M.** Patterns of hearing loss in
726 non-explosive blast injury of the ear. *J Laryngol Otol* 111: 1137–1141, 1997.
- 727 **Bharadwaj HM, Masud S, Mehraei G, Verhulst S, Shinn-Cunningham BG.**
728 Individual differences reveal correlates of hidden hearing deficits. *J Neurosci* 35:
729 2161–2172, 2015.
- 730 **Bramhall NF, Niemczak CE, Kempel SD, Billings CJ, McMillan GP.** Evoked

731 Potentials Reveal Noise Exposure–Related Central Auditory Changes Despite
732 Normal Audiograms. *Am J Audiol* 29: 152–164, 2020.

733 **Bressler S, Goldberg H, Shinn-Cunningham B.** Sensory coding and cognitive
734 processing of sound in Veterans with blast exposure. *Hear Res* 349: 98–110, 2017.

735 **Brett B, Krishnan G, Barth DS.** The effects of subcortical lesions on evoked
736 potentials and spontaneous high frequency (gamma-band) oscillating potentials in rat
737 auditory cortex. *Brain Res* 721: 155–166, 1996.

738 **Caspary DM, Ling L, Turner JG, Hughes LF.** Inhibitory neurotransmission, plasticity
739 and aging in the mammalian central auditory system. *J Exp Biol* 211: 1781–1791,
740 2008.

741 **Caspary DM, Schatteman T a, Hughes LF.** Age-related changes in the inhibitory
742 response properties of dorsal cochlear nucleus output neurons: role of inhibitory
743 inputs. *J Neurosci* 25: 10952–9, 2005.

744 **Cave K, Cornish EM, Chandler DW.** Blast Injury of the Ear: Clinical Update from the
745 Global War on Terror. *Mil Med* 172: 726–730, 2007.

746 **Chabot-Leclerc A, MacDonald EN, Dau T.** Predicting binaural speech intelligibility
747 using the signal-to-noise ratio in the envelope power spectrum domain. *J Acoust Soc*
748 *Am* 140: 192–205, 2016.

749 **Chavko M, Watanabe T, Adeeb S, Lankasky J, Ahlers ST, McCarron RM.**
750 Relationship between orientation to a blast and pressure wave propagation inside the
751 rat brain. *J Neurosci Methods* 195: 61–66, 2011.

752 **Cho HJ, Sajja VSSS, VandeVord PJ, Lee YW.** Blast induces oxidative stress,

753 inflammation, neuronal loss and subsequent short-term memory impairment in rats.
754 *Neuroscience* 253: 9–20, 2013a.

755 **Cho S II, Gao SS, Xia A, Wang R, Salles FT, Raphael PD, Abaya H, Wachtel J,**
756 **Baek J, Jacobs D, Rasband MN, Oghalai JS.** Mechanisms of Hearing Loss after
757 Blast Injury to the Ear. *PLoS One* 8, 2013b.

758 **Cohen JT, Ziv G, Bloom J, Zikk D, Rapoport Y, Himmelfarb MZ.** Blast injury of the
759 ear in a confined space explosion: Auditory and vestibular evaluation. *Isr Med Assoc J*
760 4: 559–562, 2002.

761 **Dal Cengio Leonardi A, Keane NJ, Bir CA, Ryan AG, Xu L, VandeVord PJ.** Head
762 orientation affects the intracranial pressure response resulting from shock wave
763 loading in the rat. *J Biomech* 45: 2595–2602, 2012.

764 **Deiber MP, Ibañez V, Fischer C, Perrin F, Mauguière F.** Sequential mapping
765 favours the hypothesis of distinct generators for Na and Pa middle latency auditory
766 evoked potentials. *Electroencephalogr Clin Neurophysiol Evoked Potentials* 71:
767 187–197, 1988.

768 **DePalma RG, Burris DG, Champion HR, Hodgson MJ.** Current concepts: Blast
769 injuries. *N. Engl. J. Med.* 352Massachusetts Medical Society: 1335–1342, 2005.

770 **Di S, Barth DS.** The functional anatomy of middle-latency auditory evoked potentials:
771 Thalamocortical connections. *J Neurophysiol* 68: 425–431, 1992.

772 **Du X, Ewert DL, Cheng W, West MB, Lu J, Li W, Floyd RA, Kopke RD.** Effects of
773 antioxidant treatment on blast-induced brain injury. *PLoS One* 8: e80138, 2013.

774 **Ewert DL, Lu J, Li W, Du X, Floyd R, Kopke R.** Antioxidant treatment reduces

775 blast-induced cochlear damage and hearing loss. *Hear Res* 285: 29–39, 2012.

776 **Gallun FJ, Diedesch AC, Kubli LR, Walden TC, Folmer RL, Samantha Lewis S,**

777 **McDermott DJ, Fausti SA, Leek MR.** Performance on tests of central auditory

778 processing by individuals exposed to high-intensity blasts. *J Rehabil Res Dev* 49:

779 1005–1024, 2012a.

780 **Gallun FJ, Lewis MS, Folmer RL, Diedesch AC, Aud ;, Kubli LR, McDermott DJ,**

781 **Walden TC, Fausti S a, Lew HL, Leek MR.** Implications of blast exposure for central

782 auditory function: a review. *J Rehabil Res Dev* 49: 1059–74, 2012b.

783 **Garman RH, Jenkins LW, Switzer RC, Bauman RA, Tong LC, Swauger P V.,**

784 **Parks SA, Ritzel D V., Dixon CE, Clark RSB, Bayir H, Kagan V, Jackson EK,**

785 **Kochanek PM.** Blast Exposure in Rats with Body Shielding Is Characterized Primarily

786 by Diffuse Axonal Injury. *J Neurotrauma* 28: 947–959, 2011.

787 **Greenhouse SW, Geisser S.** On methods in the analysis of profile data.

788 *Psychometrika* 24: 95–112, 1959.

789 **Van Haesendonck G, Van Rompaey V, Gilles A, Topsakal V, Van de Heyning P.**

790 Otologic Outcomes After Blast Injury: The Brussels Bombing Experience. *Otol*

791 *Neurotol* 39: 1250–1255, 2018.

792 **Hamann K, Durkes A, Ouyang H, Uchida K, Pond A, Shi R.** Critical role of acrolein

793 in secondary injury following ex vivo spinal cord trauma. *J Neurochem* 107: 712–721,

794 2008.

795 **Hickox AE, Liberman MC.** Is noise-induced cochlear neuropathy key to the

796 generation of hyperacusis or tinnitus? *J Neurophysiol* 111: 552–564, 2014.

797 **Hua Y, Wang Y, Gu L.** Primary blast waves induced brain dynamics influenced by
798 head orientations. *Biomed Eng Lett* 7: 253–259, 2017.

799 **Joris PX, Schreiner CE, Rees A.** *Neural Processing of Amplitude-Modulated Sounds.*
800 American Physiological Society, 2004.

801 **Kerr AG.** The effects of blast on the ear. *J Laryngol Otol* 94: 107–110, 1980.

802 **Knudsen SK, Øen EO.** Blast-induced neurotrauma in whales. *Neurosci Res* 46:
803 377–386, 2003.

804 **Krishnan A, Gandour JT, Suresh CH.** Cortical pitch response components show
805 differential sensitivity to native and nonnative pitch contours. *Brain Lang* 138: 51–60,
806 2014.

807 **Krishnan A, Gandour JT, Suresh CH.** Pitch processing of dynamic lexical tones in
808 the auditory cortex is influenced by sensory and extrasensory processes. *Eur J*
809 *Neurosci* 41: 1496–1504, 2015.

810 **Krishnan A, Gandour JT, Xu Y, Suresh CH.** Language-dependent changes in
811 pitch-relevant neural activity in the auditory cortex reflect differential weighting of
812 temporal attributes of pitch contours. *J Neurolinguistics* 41: 38–49, 2017a.

813 **Krishnan A, Suresh CH, Gandour JT.** Changes in pitch height elicit both
814 language-universal and language-dependent changes in neural representation of
815 pitch in the brainstem and auditory cortex. *Neuroscience* 346: 52–63, 2017b.

816 **Kubli LR, Brungart D, Northern J.** Effect of Blast Injury on Auditory Localization in
817 Military Service Members. *Ear Hear* 39: 457–469, 2018.

818 **Kujawa SG, Liberman MC.** Synaptopathy in the noise-exposed and aging cochlea:

819 Primary neural degeneration in acquired sensorineural hearing loss. *Hear Res* 330:
820 191–199, 2015.

821 **Lai J, Bartlett EL.** Age-related shifts in distortion product otoacoustic emissions
822 peak-ratios and amplitude modulation spectra. *Hear Res* 327: 186–198, 2015.

823 **Lai J, Bartlett EL.** Masking Differentially Affects Envelope-following Responses in
824 Young and Aged Animals. *Neuroscience* 386: 150–165, 2018.

825 **Lai J, Sommer AL, Bartlett EL.** Age-related changes in envelope-following
826 responses at equalized peripheral or central activation. *Neurobiol Aging* 58: 191–200,
827 2017.

828 **Laplaca MC, Lee VMY, Thibault LE.** An in vitro model of traumatic neuronal injury:
829 Loading rate-dependent changes in acute cytosolic calcium and lactate
830 dehydrogenase release. *J Neurotrauma* 14: 355–368, 1997.

831 **Leung LY, VandeVord PJ, Dal Cengio AL, Bir C, Yang KH, King AI.** Blast related
832 neurotrauma: A review of cellular injury. *MCB Mol Cell Biomech* 5: 155–168, 2008.

833 **Lew HL, Garvert DW, Pogoda TK, Hsu P Te, Devine JM, White DK, Myers PJ,**
834 **Goodrich GL.** Auditory and visual impairments in patients with blast-related traumatic
835 brain injury: Effect of dual sensory impairment on functional independence measure. *J*
836 *Rehabil Res Dev* 46: 819–826, 2009.

837 **Liberman MC.** Noise-induced and age-related hearing loss: New perspectives and
838 potential therapies. *F1000Research* 6: 1–11, 2017.

839 **Liégeois-Chauvel C, Musolino A, Badier JM, Marquis P, Chauvel P.** Evoked
840 potentials recorded from the auditory cortex in man: evaluation and topography of the

841 middle latency components. *Electroencephalogr Clin Neurophysiol Evoked Potentials*
842 92: 204–214, 1994.

843 **Luo H, Pace E, Zhang X, Zhang J.** Blast-Induced tinnitus and spontaneous firing
844 changes in the rat dorsal cochlear nucleus. *J Neurosci Res* 92: 1466–1477, 2014a.

845 **Luo H, Pace E, Zhang X, Zhang J.** Blast-induced tinnitus and spontaneous activity
846 changes in the rat inferior colliculus. *Neurosci Lett* 580: 47–51, 2014b.

847 **Mahmood G, Mei Z, Hojjat H, Pace E, Kallakuri S, Zhang JS.** Therapeutic effect of
848 sildenafil on blast-induced tinnitus and auditory impairment. *Neuroscience* 269:
849 367–382, 2014.

850 **Mao JC, Pace E, Pierozynski P, Kou Z, Shen Y, Vandevord P, Haacke EM, Zhang**
851 **X, Zhang J.** Blast-induced tinnitus and hearing loss in rats: Behavioral and imaging
852 assays. *J Neurotrauma* 29: 430–444, 2012.

853 **Masri S, Zhang LS, Luo H, Pace E, Zhang J, Bao S.** Blast Exposure Disrupts the
854 Tonotopic Frequency Map in the Primary Auditory Cortex. *Neuroscience* 379:
855 428–434, 2018.

856 **McGee T, Kraus N.** Auditory development reflected by middle latency response. *Ear*
857 *Hear* 17: 419–429, 1996.

858 **McGee T, Kraus N, Comperatore C, Nicol T.** Subcortical and cortical components of
859 the MLR generating system. *Brain Res* 544: 211–220, 1991.

860 **McGee T, Kraus N, Littman T, Nicol T.** Contributions of medial geniculate body
861 subdivisions to the middle latency response. *Hear Res* 61: 147–154, 1992.

862 **Meehan A, Hebert D, Deru K, Weaver LK.** Longitudinal study of hyperbaric oxygen

863 intervention on balance and affective symptoms in military service members with
864 persistent post-concussive symptoms. *J Vestib Res Equilib Orientat* 29: 205–219,
865 2019.

866 **Musiek F, Nagle S.** The middle latency response: A review of findings in various
867 central nervous system lesions. *J. Am. Acad. Audiol.* 29 American Academy of
868 Audiology: 855–867, 2018.

869 **Parthasarathy A, Bartlett E.** Two-channel recording of auditory-evoked potentials to
870 detect age-related deficits in temporal processing. *Hear Res* 289: 52–62, 2012.

871 **Parthasarathy A, Bartlett EL.** Age-related auditory deficits in temporal processing in
872 F-344 rats. *Neuroscience* 192: 619–630, 2011.

873 **Parthasarathy A, Cunningham PA, Bartlett EL.** Age-related differences in auditory
874 processing as assessed by amplitude-modulation following responses in quiet and in
875 noise. *Front Aging Neurosci* 2: 3389, 2010.

876 **Parthasarathy A, Datta J, Torres JAL, Hopkins C, Bartlett EL.** Age-related
877 changes in the relationship between auditory brainstem responses and
878 envelope-following responses. *JARO - J Assoc Res Otolaryngol* 15: 649–661, 2014.

879 **Parthasarathy A, Kujawa SG.** Synaptopathy in the aging cochlea: Characterizing
880 early-neural deficits in auditory temporal envelope processing. *J Neurosci* 38:
881 7108–7119, 2018.

882 **Patterson JH, Hamernik RP.** Blast overpressure induced structural and functional
883 changes in the auditory system. 1997.

884 **Peter V, Wong K, Narne VK, Sharma M, Purdy SC, McMahon C.** Assessing

885 spectral and temporal processing in children and adults using Temporal Modulation

886 Transfer Function (TMTF), Iterated Ripple Noise (IRN) perception, and Spectral

887 Ripple Discrimination (SRD). *J Am Acad Audiol* 25: 210–218, 2014.

888 **Phillips DJ, Schei JL, Meighan PC, Rector DM.** State-Dependent Changes in

889 Cortical Gain Control as Measured by Auditory Evoked Responses to Varying

890 Intensity Stimuli. *Sleep* 34: 1527–1537, 2011.

891 **Plack CJ, Barker D, Prendergast G.** Perceptual consequences of “hidden” hearing

892 loss. *Trends Hear* 18: 233121651455062, 2014.

893 **Rabang CF, Parthasarathy A, Venkataraman Y, Fisher ZL, Gardner SM, Bartlett**

894 **EL.** A computational model of inferior colliculus responses to amplitude modulated

895 sounds in young and aged rats. *Front Neural Circuits* 6: 77, 2012.

896 **Race N, Lai J, Shi R, Bartlett EL.** Differences in postinjury auditory system

897 pathophysiology after mild blast and nonblast acute acoustic trauma. *J Neurophysiol*

898 118: 782–799, 2017.

899 **Rafaels K, “Dale” Bass CR, Salzar RS, Panzer MB, Woods W, Feldman S,**

900 **Cummings T, Capehart B.** Survival Risk Assessment for Primary Blast Exposures to

901 the Head. *J Neurotrauma* 28: 2319–2328, 2011.

902 **Remenschneider AK, Lookabaugh S, Aliphas A, Brodsky JR, Devaiah AK,**

903 **Dagher W, Grundfast KM, Heman-Ackah SE, Rubin S, Sillman J, Tsai AC,**

904 **Vecchiotti M, Kujawa SG, Lee DJ, Quesnel AM.** Otologic outcomes after blast injury:

905 The Boston Marathon experience. *Otol Neurotol* 35: 1825–1834, 2014.

906 **Ritenour AE, Wickley A, Ritenour JS, Kriete BR, Blackbourne LH, Holcomb JB,**

- 907 **Wade CE.** Tympanic membrane perforation and hearing loss from blast overpressure
908 in Operation Enduring Freedom and Operation Iraqi Freedom wounded. *J Trauma* 64,
909 2008.
- 910 **Rosen S.** Temporal information in speech: acoustic, auditory and linguistic aspects.
911 *Philos. Trans. R. Soc. Lond. B. Biol. Sci.* 336The Royal Society London: 367–373,
912 1992.
- 913 **Säljö A, Mayorga M, Bolouri H, Svensson B, Hamberger A.** Mechanisms and
914 pathophysiology of the low-level blast brain injury in animal models. *Neuroimage* 54:
915 S83–S88, 2011.
- 916 **Saunders GH, Frederick MT, Arnold M, Silverman S, Chisolm TH, Myers P.**
917 Auditory difficulties in blast-exposed veterans with clinically normal hearing. *J Rehabil*
918 *Res Dev* 52: 343–360, 2015.
- 919 **Simpson G V., Knight RT, Brailowsky S, Prospero-Garcia O, Scabini D.** Altered
920 peripheral and brainstem auditory function in aged rats. *Brain Res* 348: 28–35, 1985.
- 921 **Simpson MIG, Prendergast G.** Auditory magnetic evoked responses. In: *Handbook*
922 *of Clinical Neurophysiology*. 2013, p. 253–270.
- 923 **Skoe E, Kraus N.** Auditory Brain Stem Response to Complex Sounds: A Tutorial. *Ear*
924 *Hear* 31: 302–324, 2010.
- 925 **Song S, Race NS, Kim A, Zhang T, Shi R, Ziaie B.** A Wireless Intracranial Brain
926 Deformation Sensing System for Blast-Induced Traumatic Brain Injury. *Sci Rep* 5:
927 1–10, 2015.
- 928 **Šuta D, Rybalko N, Pelánová J, Popelář J, Syka J.** Age-related changes in auditory

temporal processing in the rat. *Exp Gerontol* 46: 739–746, 2011.

Swaminathan J, Krishnan A, Gandour JT. Pitch encoding in speech and nonspeech contexts in the human auditory brainstem. *Neuroreport* 19: 1163–1167, 2008.

Thompson W, Marozeau J. Auditory Stream Segregation: Boundaries. In: *Music in the Social and Behavioral Sciences: An Encyclopedia*. 2014.

Tichko P, Skoe E. Frequency-dependent fine structure in the frequency-following response: The byproduct of multiple generators. *Hear Res* 348: 1–15, 2017.

Tukey JW. Comparing Individual Means in the Analysis of Variance. *Biometrics* 5: 99, 1949.

Unnikrishnan G, Mao H, Sundaramurthy A, Bell ED, Yeoh S, Monson K, Reifman J. A 3-D Rat Brain Model for Blast-Wave Exposure: Effects of Brain Vasculature and Material Properties. *Ann Biomed Eng* 47: 2033–2044, 2019.

Valderrama JT, Beach EF, Yeend I, Sharma M, Van Dun B, Dillon H. Effects of lifetime noise exposure on the middle-age human auditory brainstem response, tinnitus and speech-in-noise intelligibility. *Hear Res* 365: 36–48, 2018.

Viana LM, O'Malley JT, Burgess BJ, Jones DD, Oliveira CACP, Santos F, Merchant SN, Liberman LD, Liberman MC. Cochlear neuropathy in human presbycusis: Confocal analysis of hidden hearing loss in post-mortem tissue. *Hear Res* 327: 78–88, 2015.

Wagner L, Plontke SK, Rahne T. Perception of Iterated Rippled Noise Periodicity in Cochlear Implant Users. *Audiol Neurotol* 22: 104–115, 2017.

951 **Walls MK, Race N, Zheng L, Vega-Alvarez SM, Acosta G, Park J, Shi R.** Structural
952 and biochemical abnormalities in the absence of acute deficits in mild primary
953 blast-induced head trauma. *J Neurosurg* 124: 675–686, 2016.

954 **Walton JP.** Timing is everything: Temporal processing deficits in the aged auditory
955 brainstem. *Hear Res* 264: 63–69, 2010.

956 **Wang H, Turner JG, Ling L, Parrish JL, Hughes LF, Caspary DM.** Age-related
957 changes in glycine receptor subunit composition and binding in dorsal cochlear
958 nucleus. *Neuroscience* 160: 227–239, 2009.

959 **Wang X, Lu T, Bendor D, Bartlett E.** Neural coding of temporal information in
960 auditory thalamus and cortex. *Neuroscience* 154: 294–303, 2008.

961 **Yost WA.** Pitch of iterated rippled noise. *J Acoust Soc Am* 100: 511–518, 1996a.
962 **Yost WA.** Pitch strength of iterated rippled noise. *J Acoust Soc Am* 100: 3329–3335,
963 1996b.

964
965

966 **Fig 1. Auditory evoked potential experiment setup and examples of ABR**

967 **waveforms.** A) Electrode placement and channel configuration of the study's
968 auditory evoked potential experiment. B) Examples of ABR waveforms of a
969 pre-exposure animal, at 80 dB SPL and 30 dB SL, with relevant wave peaks labeled.
970 The waves for which amplitudes are measured are labeled with a black triangle.

971

972 **Fig 2. ABR threshold changes of Blast (N=10) and Sham (N=6) rats during the**

973 **first two months post-exposure.** Blast animals demonstrated drastic increases
974 (worse) of Click, 8 kHz, and 16 kHz thresholds (red lines) post-exposure as opposed
975 to Sham animals (blue lines). Significant main effects ($p \leq 0.001$) of Groups and
976 Group*Time interactions were observed in all carriers. Significant Simple Main Effect
977 of single time points observed in various carriers throughout the two months. For
978 subsequent figures, red lines will denote blast-exposed animals, and blue lines will
979 denote sham-exposed animals. Asterisks indicate time points where significant
980 Simple Main Effects of Group was demonstrated (Supp. Table 1):

981 ***Blast threshold significantly higher than Sham in Click, 8kHz, and 16kHz, $p < 0.05$;

982 **Blast threshold significantly higher only in Click and 16 kHz;

983 *Blast threshold significantly higher only in Click.

984

985 **Fig 3. ABR wave I, III, and V amplitudes of Blast (N=10) and Sham (N=6) rats**

986 **during the first two months post-exposure expose persistent blast-induced**

987 **differences at 80 dB SPL.** Significant main Group*Time interaction effects ($p \leq 0.001$)

988 observed in waves I (left column), III (center column), and V (right column) for all
 989 carriers: A) Click ABR; B) 8 kHz ABR; C) 16 kHz ABR. Click ABR revealed
 990 blast-induced reduction of ABR wave amplitudes to a greater degree than both tone
 991 ABRs. Later waves (Wave III and V) showed earlier recovery in Blast animals.
 992 *Significant Simple Main Effect of Group in ABR Wave Amplitudes, $p < 0.05$.

993

994 **Fig 4. ABR wave I, III, and V amplitudes of Blast (N=10) and Sham (N=6) rats**
 995 **during the first two months post-exposure at 30 dB SL.** Similar format to Fig. 3.
 996 Significant main Group*Time interaction effects only observed with Click ABR waves
 997 (Wave I: $p = 0.016$; Wave III: $p = 0.04$; Wave V: $p = 0.003$) A) Click ABR; B) 8 kHz ABR;
 998 C) 16 kHz ABR.

999 *Significant Simple Main Effect of Group in ABR Wave Amplitudes, $p < 0.05$.

1000

1001 **Fig 5. MLR waveforms and peak amplitudes of Blast (N=8) and Sham (N=6) rats**
 1002 **during the first two months post-exposure at 80 dB SPL and at 30 dB SL**
 1003 **(Thresh + 30 dB).** Grand average traces of Click MLR waveforms at 80 dB SPL: A)
 1004 Blast, pre-blast to day 7. Arrowheads indicate measured peaks in E-H; B) Sham,
 1005 pre-blast to day 7; C) Blast, day 10 to day 60; D) Sham, day 10 to day 60.
 1006 Normalized Click MLR wave amplitudes over time: E) Blast, 80 dB SPL; F) Sham, 80
 1007 dB SPL; G) Blast, 30 dB SL; H) Blast, 30 dB SL.

1008 *Significant difference in normalized wave P1, N1 and P2 amplitudes compared to
 1009 pre-exposure, $p < 0.05$.

1010 †Significant difference in normalized wave N1 amplitudes only, $p < 0.05$.

1011 ‡Significant difference in normalized wave N1 and P2 amplitude, $p < 0.05$.

1012

1013 **Fig 6. AM depth stimuli and EFR responses from Blast (N=10) and Sham (N=6)**

1014 **rats during the first two months post-exposure at 30 dB above threshold, in**

1015 **quiet.** A) AM depth stimulus waveforms at 100% and 50% modulation depths; B)

1016 nSAM FFT amplitudes at 10 Hz (left), 45 Hz (center), and 256 Hz (right). Significant

1017 Group effect at 45Hz ($p = 0.007$); Similar format in C and D. C) SAM 8 kHz FFT

1018 amplitudes at 45 Hz show a steady yet insignificant increase in later short-term (day

1019 7-14); D) SAM 16k FFT amplitudes found no significant Group effect.

1020 **Significant Simple Main Effect of Group in FFT Amplitudes in both 100% depth and

1021 50% depth

1022 * Significant Simple Main Effect of Group in FFT Amplitudes only in 100% depth

1023

1024 **Fig 7. AM noise stimuli and EFR responses from Blast (N=10) and Sham (N=6)**

1025 **rats during the first two months post-exposure at 30 dB above threshold,**

1026 **modulation depth 100%.** A) AM noise stimulus composition and waveform. B)

1027 Amplitude modulated noise carrier. FFT amplitudes at signal modulation frequency in

1028 quiet and with 71 Hz AM noise masker level of 20SNR or 0SNR (equal) show

1029 significant Noise * Group effect for: B) nSAM noise at 45 Hz ($p = 0.011$) modulation

1030 frequency; C) SAM 8 kHz noise at 10 Hz ($p = 0.001$) and 45 Hz ($p = 0.015$) modulation

1031 frequency.

1032 * Significant Simple Main Effect of Group

1033

1034 **Fig 8. IRN Chinese Tone stimuli and responses from Blast (N=8) and Sham**

1035 **(N=6) rats during the first two months post-exposure at 30 dB above threshold,**

1036 **32 iterations. A) Example waveform and spectrogram of IRN Tone 2 stimulus; B)**

1037 **Examples of Peak Frequency of IRN Evoked Potential in Pre-blast (score: Tone**

1038 **2=36/51, Tone 4=39/51) and Post-blast Brain (day 10 post-blast, score: Tone**

1039 **2=21/51, Tone 4=18/51) from an individual animal; C) Significant effect of Group (*)**

1040 **was seen in IRN Tone 2 (top, $p=0.026$) and Tone 4 (bottom, $p=0.029$) pitch-tracking**

1041 **score, though Simple Main Effect of is limited for individual time points; D)**

1042 **Cross-correlation of post-blast IRN responses to corresponding pre-blast responses.**

1043 **Significant differences (*) in correlation coefficients to pre-blast responses between**

1044 **Blast and Sham were observed in two waves: day 1-10, and day 30 ($p<0.05$, paired**

1045 **sign-rank).**

1046

1047 **Fig 9. Pitch tracking scores of responses to IRN Tone 2 stimuli with pitch**

1048 **salience controlled by altering iteration number at different time points, at 30**

1049 **dB above threshold. Though the effect of Iterations on pitch-tracking score was**

1050 **significant ($p<0.001$), no significant Iteration * Group interaction was observed.**

1051

1052 **Table 1. Summary of 80 dB SPL ABR Wave I, III and V repeated measure ABR**

1053 **statistics.**

1054

1055 **Table 2. Summary of 30 dB SL ABR Wave I, III and V repeated measure ABR**
 1056 **statistics.**

1057

1058 **Table 3. Simple main effects of Group on ABR wave amplitudes over time.**

1059 Post-blast ABR amplitudes of Blast (N=10) and Sham (N=6) groups are compared
 1060 using rmANOVA at each time point recorded. A $p < 0.05$ showed significant simple
 1061 main effect of Group at that time point.

1062

1063 **Table 4. Summary of post hoc tests against pre-blast ABR amplitudes.**

1064 Post-blast ABR amplitudes of Blast (N=10) and Sham (N=6) are compared against
 1065 pre-blast amplitudes of the same group to show blast impact and recovery.

1066

1067 **Table 5. Simple main effects of Group on click MLR wave amplitudes at 80 dB**

1068 **SPL over time.** Post-blast click MLR amplitudes of Blast (N=8) and Sham (N=6)
 1069 groups at 80 dB SPL are compared using rmANOVA at each time point recorded. A
 1070 $p < 0.05$ showed significant simple main effect of Group at that time point.

1071

1072 **Table 1**

80dB SPL ABR			df	F	p	η^2_p
Click	Wave I	Time	4.163	9.980	< .001	0.416
		Group	1.000	23.080	< .001	0.622
		Time * Group	4.163	11.685	< .001	0.455
	Wave III	Time	3.641	11.065	< .001	0.441
		Group	1.000	17.207	< .001	0.551
		Time * Group	3.641	8.871	< .001	0.388
	Wave V	Time	4.000	14.134	< .001	0.502
		Group	1.000	23.203	< .001	0.624
		Time * Group	4.000	10.990	< .001	0.440
8 kHz	Wave I	Time	4.413	8.102	< .001	0.367
		Group	1.000	14.409	0.002	0.507
		Time * Group	4.413	11.760	< .001	0.457
	Wave III	Time	3.378	14.084	< .001	0.501
		Group	1.000	6.266	0.025	0.309
		Time * Group	3.378	13.826	< .001	0.497
	Wave V	Time	3.908	8.545	< .001	0.379
		Group	1.000	9.859	0.007	0.413
		Time * Group	3.908	9.346	< .001	0.400
16 kHz	Wave I	Time	3.534	9.845	< .001	0.413
		Group	1.000	27.486	< .001	0.663
		Time * Group	3.534	14.328	< .001	0.506
	Wave III	Time	3.055	9.845	< .001	0.413
		Group	1.000	13.048	0.003	0.482
		Time * Group	3.055	14.328	< .001	0.506
	Wave V	Time	3.933	8.838	< .001	0.387
		Group	1.000	20.528	< .001	0.595
		Time * Group	3.933	10.066	< .001	0.418

1073

1074

1075 **Table 2**

30dB SL ABR			df	F	p	η^2_p
Click	Wave I	Time	4.360	2.554	0.043	0.154
		Group	1.000	3.637	0.077	0.206
		Time * Group	4.360	2.630	0.039	0.158
	Wave III	Time	3.878	2.544	0.052	0.154
		Group	1.000	1.811	0.200	0.115
		Time * Group	3.878	2.720	0.040	0.163
	Wave V	Time	4.784	2.568	0.037	0.155
		Group	1.000	1.479	0.244	0.096
		Time * Group	4.784	3.429	0.009	0.197
8 kHz	Wave I	Time	4.264	3.146	0.018	0.183
		Group	1.000	6.852e ⁻⁵	0.994	0.000
		Time * Group	4.264	0.200	0.945	0.014
	Wave III	Time	3.414	2.432	0.069	0.148
		Group	1.000	0.020	0.889	0.001
		Time * Group	3.414	1.184	0.328	0.078
	Wave V	Time	3.912	1.837	0.136	0.116
		Group	1.000	0.361	0.558	0.025
		Time * Group	3.912	0.618	0.648	0.042
16 kHz	Wave I	Time	4.469	2.325	0.031	0.142
		Group	1.000	1.046	0.324	0.070
		Time * Group	4.469	2.381	0.027	0.145
	Wave III	Time	3.160	0.562	0.651	0.039
		Group	1.000	1.149	0.302	0.076
		Time * Group	3.160	1.930	0.136	0.121
	Wave V	Time	4.874	1.160	0.338	0.077
		Group	1.000	4.905e ⁻⁴	0.983	0.000
		Time * Group	4.874	1.646	0.161	0.105

1076

1077

1078 **Table 3**

Simple Main Effects			80 dB SPL			30dB SL		
		Time	Mean square	F	p	Mean Square	F	p
Click	Wave I	day1	13.942	31.329	< .001	2.097	8.019	0.013
		day4	12.438	30.917	< .001	1.843	7.730	0.015
		day7	4.081	18.418	< .001	0.024	0.102	0.754
		day10	1.601	7.023	0.019	0.020	0.127	0.726
		day14	3.180	10.008	0.007	0.596	3.044	0.103
		day30	1.517	8.285	0.012	0.184	1.829	0.198
		day60	1.013	4.393	0.055	0.102	0.632	0.440
	Wave III	day1	9.708	30.148	< .001	1.977	6.629	0.022
		day4	5.754	23.070	< .001	0.692	3.416	0.086
		day7	3.725	33.967	< .001	0.470	3.917	0.068
		day10	1.690	11.712	0.004	0.093	0.665	0.429
		day14	0.854	8.587	0.011	0.039	0.474	0.502
		day30	0.634	4.714	0.048	0.005	0.088	0.771
		day60	0.064	0.315	0.584	0.029	0.219	0.647
	Wave V	day1	17.134	45.066	< .001	3.596	9.213	0.009
		day4	14.672	35.376	< .001	2.178	8.580	0.011
		day7	4.419	13.382	0.003	0.056	0.132	0.722
		day10	2.264	8.415	0.012	0.012	0.043	0.839
		day14	4.709	16.223	0.001	0.104	0.347	0.565
		day30	1.214	3.651	0.077	0.009	0.028	0.870
		day60	0.414	1.155	0.301	0.002	0.007	0.934
8 kHz	Wave I	day1	7.136	45.959	< .001	0.000	0.004	0.948
		day4	6.915	37.954	< .001	0.001	0.014	0.909
		day7	1.892	15.704	0.001	0.017	0.551	0.470
		day10	0.754	2.693	0.123	0.014	0.159	0.696
		day14	0.803	4.657	0.049	0.010	0.096	0.762
		day30	0.421	2.532	0.134	0.001	0.015	0.904
		day60	0.285	1.562	0.232	0.006	0.450	0.513
	Wave III	day1	5.977	37.898	< .001	0.084	0.838	0.375
		day4	4.139	36.832	< .001	0.000	0.000	0.984
		day7	3.544	23.802	< .001	0.034	0.703	0.416
		day10	0.990	5.847	0.030	0.017	0.232	0.637
		day14	0.167	0.851	0.372	0.055	1.274	0.278
		day30	0.022	0.131	0.722	0.041	0.301	0.592
		day60	0.167	0.640	0.437	0.062	1.420	0.253
	Wave V	day1	6.374	100.269	< .001	0.020	0.135	0.719
		day4	4.459	28.229	< .001	0.005	0.165	0.691
		day7	1.580	11.078	0.005	0.129	3.798	0.072
		day10	0.392	2.043	0.175	0.104	1.256	0.281

16 kHz	Wave I	day14	0.449	3.269	0.092	0.001	0.010	0.924
		day30	0.006	0.026	0.875	0.018	0.149	0.705
		day60	0.017	0.060	0.811	0.007	0.187	0.672
		day1	5.090	40.130	< .001	0.205	2.470	0.138
		day4	5.910	61.374	< .001	0.026	0.827	0.378
		day7	2.397	29.278	< .001	0.090	2.321	0.150
	Wave III	day10	0.723	4.602	0.050	0.009	0.305	0.590
		day14	1.766	24.888	< .001	0.009	0.153	0.701
		day30	0.515	6.551	0.023	0.000	0.000	0.992
		day60	0.205	2.242	0.156	0.022	1.009	0.332
		day1	3.592	39.592	< .001	0.205	2.470	0.138
		day4	2.919	38.728	< .001	0.026	0.827	0.378
	Wave V	day7	2.507	35.072	< .001	0.090	2.321	0.150
		day10	0.965	11.997	0.004	0.009	0.305	0.590
		day14	0.676	8.374	0.012	0.009	0.153	0.701
		day30	0.253	3.337	0.089	0.000	0.000	0.992
		day60	0.006	0.056	0.816	0.022	1.009	0.332
		day1	4.772	37.802	< .001	0.118	1.617	0.224
		day4	3.414	44.163	< .001	0.000	0.005	0.945
		day7	2.150	21.095	< .001	0.066	1.575	0.230
		day10	0.902	7.214	0.018	0.000	0.002	0.961
		day14	1.283	15.210	0.002	0.017	0.336	0.571
		day30	0.100	0.888	0.362	0.103	1.301	0.273
		day60	0.019	0.293	0.597	0.079	1.541	0.235

Table 4

			80dB SPL							30dB SL						
			day1	day4	day7	day10	day14	day30	day60	day1	day4	day7	day10	day14	day30	day60
Click	Wave I	Blast Sha m	<0.001	<0.001	<0.001	<0.001	<0.001	<0.001	<0.001	0.001	0.244	1.000	1.000	1.000	0.300	0.808
			1.000	1.000	1.000	1.000	1.000	0.984	0.999	1.000	1.000	1.000	1.000	1.000	0.997	1.000
	Wave III	Blast Sha m	<0.001	<0.001	<0.001	<0.001	<0.001	<0.001	0.002	0.003	0.015	0.780	0.285	0.934	0.528	0.797
			1.000	0.916	1.000	0.915	0.902	0.838	0.600	1.000	1.000	1.000	0.966	0.767	0.854	0.652
	Wave V	Blast Sha m	<0.001	<0.001	<0.001	<0.001	<0.001	<0.001	<0.001	0.009	0.440	1.000	1.000	1.000	1.000	1.000
			1.000	1.000	1.000	1.000	1.000	0.990	0.997	1.000	1.000	1.000	1.000	1.000	0.967	1.000
8 kHz	Wave I	Blast Sha m	<0.001	<0.001	<0.001	0.129	0.525	0.575	0.008	0.840	0.996	1.000	1.000	1.000	1.000	0.943
			0.978	1.000	0.998	1.000	1.000	1.000	0.972	0.957	0.999	1.000	1.000	1.000	1.000	1.000
	Wave III	Blast Sha m	<0.001	<0.001	<0.001	<0.001	<0.001	<0.023	0.878	0.998	1.000	1.000	1.000	1.000	1.000	1.000
			1.000	0.996	1.000	1.000	0.968	1.000	0.999	0.995	1.000	1.000	0.998	0.932	1.000	0.932
	Wave V	Blast Sha m	<0.001	<0.001	<0.001	0.993	0.994	1.000	1.000	0.902	1.000	1.000	1.000	1.000	1.000	1.000
			1.000	1.000	0.991	1.000	1.000	1.000	0.974	1.000	1.000	0.998	1.000	1.000	1.000	0.999

16 kHz	Wave I	Blast Sha m	<0.001	<0.001	<0.001	<0.001	0.050	0.020	<0.001	1.000	1.000	1.000	1.000	1.000	1.000	0.999
			1.000	0.993	0.997	0.965	1.000	1.000	0.149	0.296	0.999	1.000	1.000	1.000	1.000	0.973
	Wave III	Blast Sha m	<0.001	<0.001	<0.001	<0.001	<0.001	<0.001	<0.001	1.000	1.000	1.000	1.000	0.993	1.000	0.930
			1.000	0.990	0.973	0.534	0.805	0.838	0.203	1.000	0.982	1.000	0.994	0.880	0.938	0.890
	Wave V	Blast Sha m	<0.001	<0.001	<0.001	<0.001	0.031	0.879	0.063	1.000	1.000	1.000	1.000	0.998	1.000	1.000
			1.000	1.000	0.899	0.520	1.000	0.915	0.031	1.000	1.000	1.000	1.000	1.000	0.986	0.843

Table 5

	P1				N1				P2				N2			
Time	df	Mean Square	F	p	df	Mean Square	F	p	df	Mean Square	F	p	df	Mean Square	F	p
day1	1	0.028	5.91	0.032	1	0.037	25.608	< .001	1	0.009	6.039	0.03	1	0.003	1.404	0.259
day4	1	0.018	3.168	0.1	1	0.027	11.332	0.006	1	0.012	11.61	0.005	1	0.011	4.666	0.052
day7	1	0.024	7.68	0.017	1	0.002	3.953	0.07	1	0.001	1.446	0.252	1	1.950e ⁻⁶	9.167e ⁻⁴	0.976
day10	1	0.002	0.655	0.434	1	0.004	4.249	0.062	1	0.001	1.255	0.284	1	4.433e ⁻⁵	0.015	0.904
day14	1	0.008	2.302	0.155	1	0.007	6.569	0.025	1	0.005	4.15	0.064	1	1.140e ⁻⁴	0.02	0.89
day30	1	9.435e ⁻⁵	0.028	0.869	1	0.002	0.514	0.487	1	2.632e ⁻⁵	0.011	0.918	1	9.054e ⁻⁶	0.002	0.961
day60	1	1.338e ⁻⁴	0.03	0.866	1	0.005	3.334	0.093	1	0.003	2.787	0.121	1	0.018	8.122	0.015

1086

Supplementary Table 1

	Click				8 kHz				16 kHz			
Time	df	Mean Square	F	p	df	Mean Square	F	p	df	Mean Square	F	p
day1	1	2375.104	42.314	< .001	1	2343.75	23.438	< .001	1	2666.667	16.35	0.001
day4	1	2633.438	61.192	< .001	1	1926.667	98.683	< .001	1	3720.937	40.777	< .001
day7	1	1306.667	94.621	< .001	1	700.417	19.877	< .001	1	1377.604	21.529	< .001
day10	1	825.104	37.163	< .001	1	192.604	3.151	0.098	1	617.604	17.093	0.001
day14	1	570.417	46.072	< .001	1	33.75	0.583	0.458	1	700.417	16.527	0.001
day30	1	303.75	10.904	0.005	1	23.437	0.228	0.64	1	158.438	2.948	0.108
day60	1	166.667	12.727	0.003	1	0.104	0.004	0.95	1	150.417	3.549	0.081

1087

1088

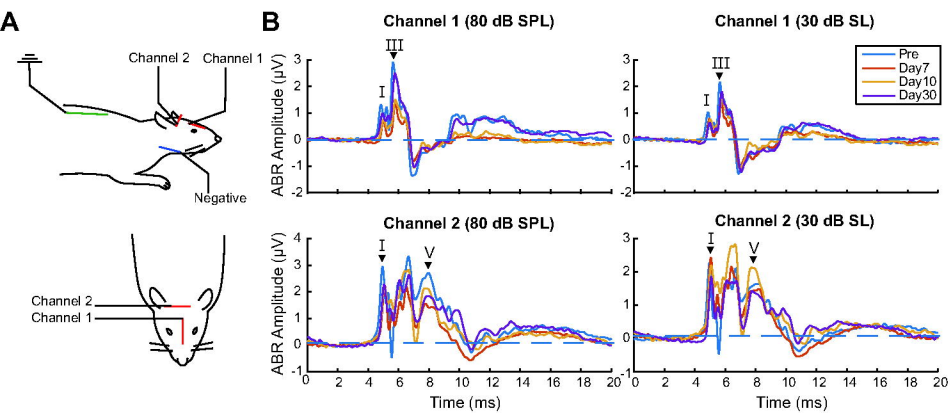
1089

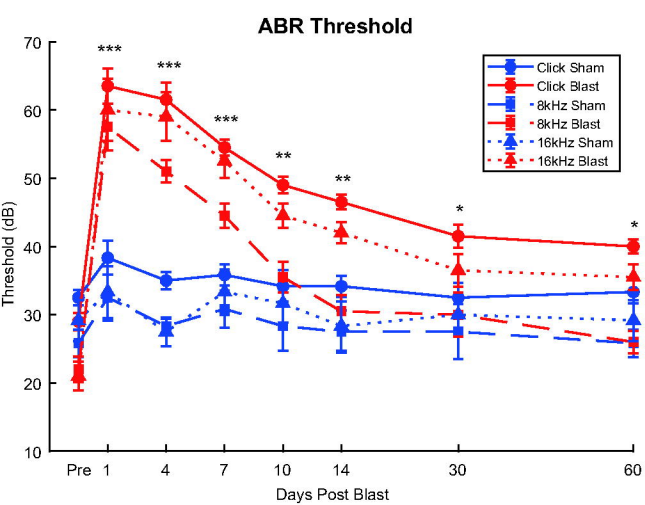
1090

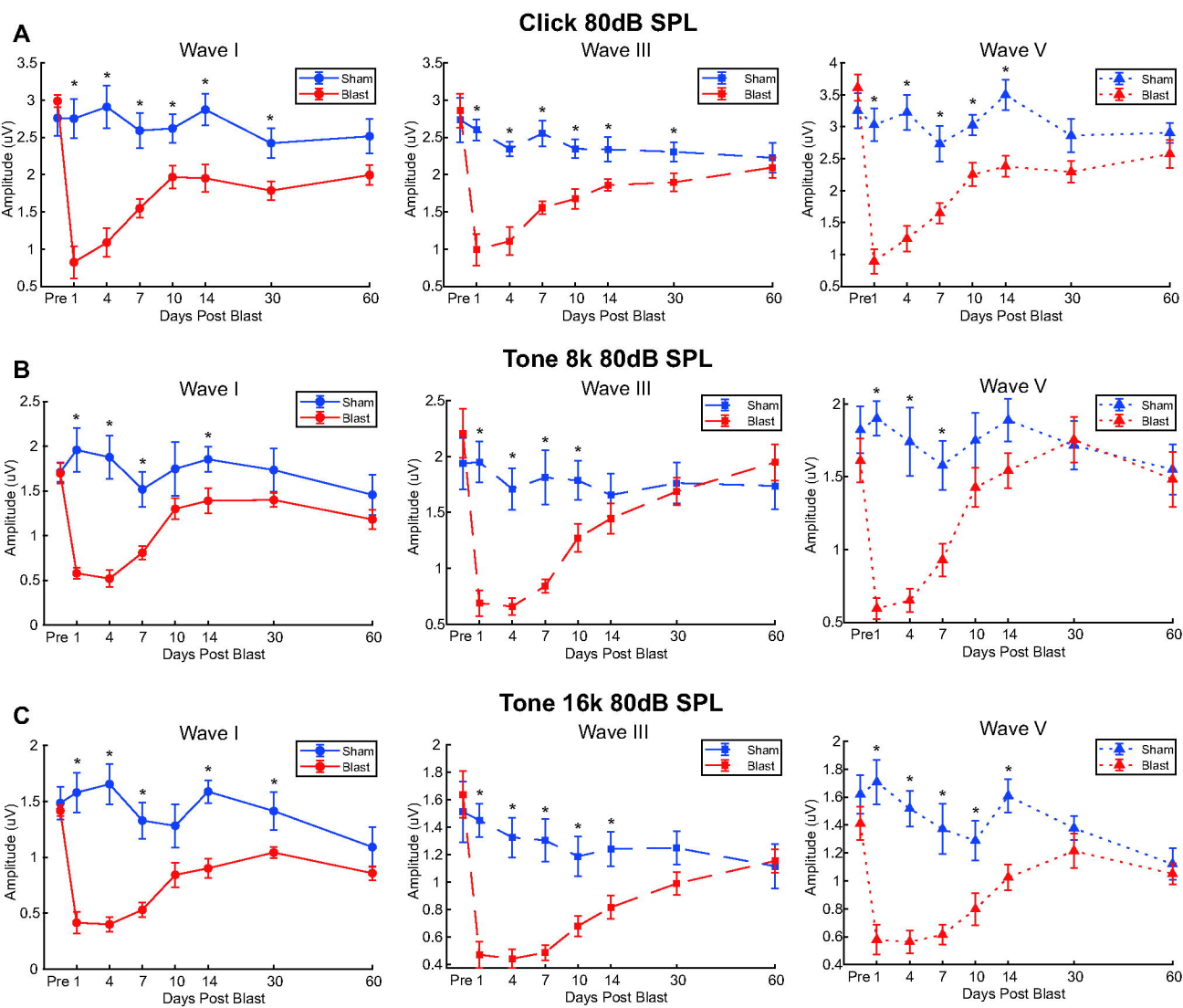
1091

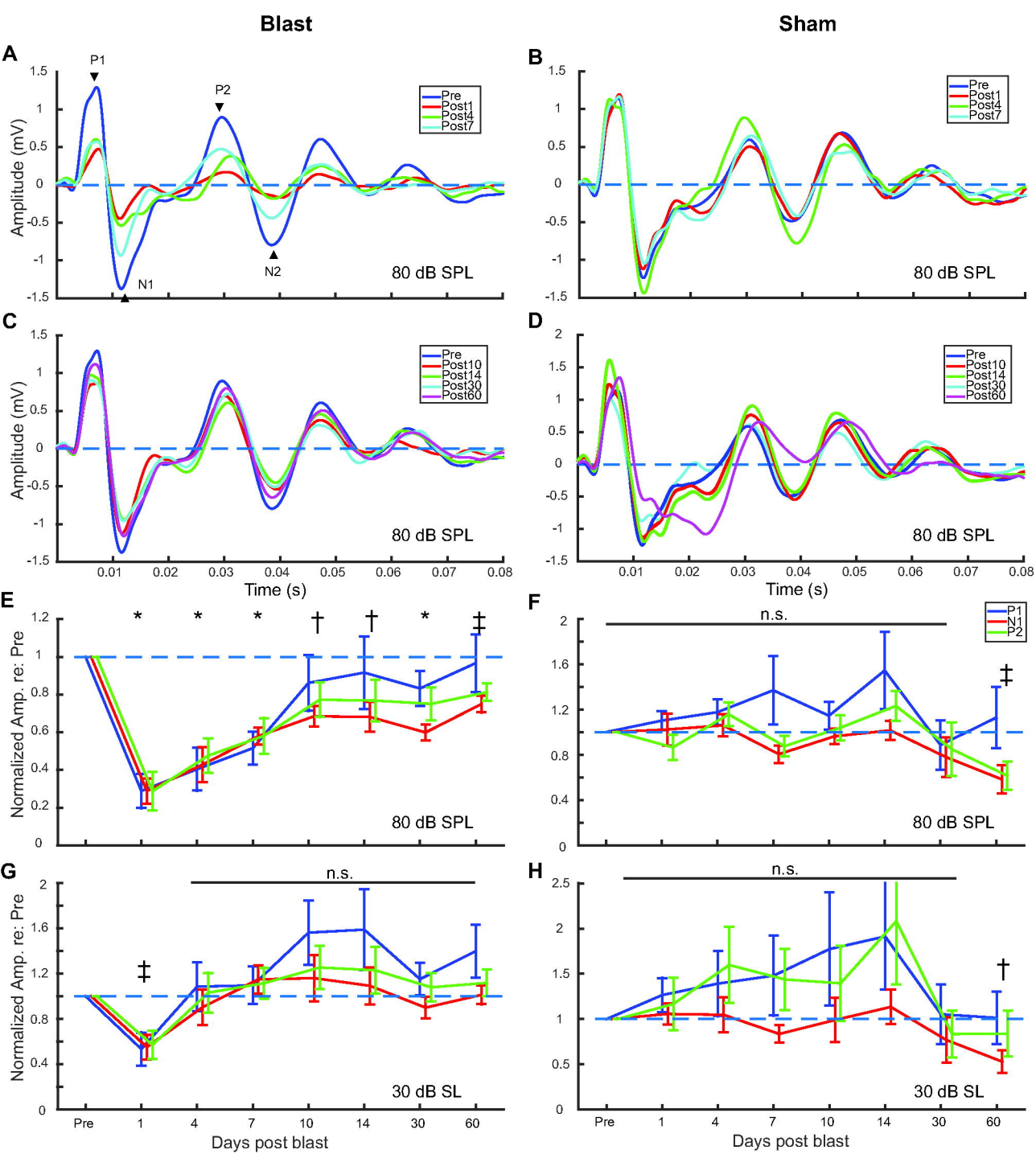
1092

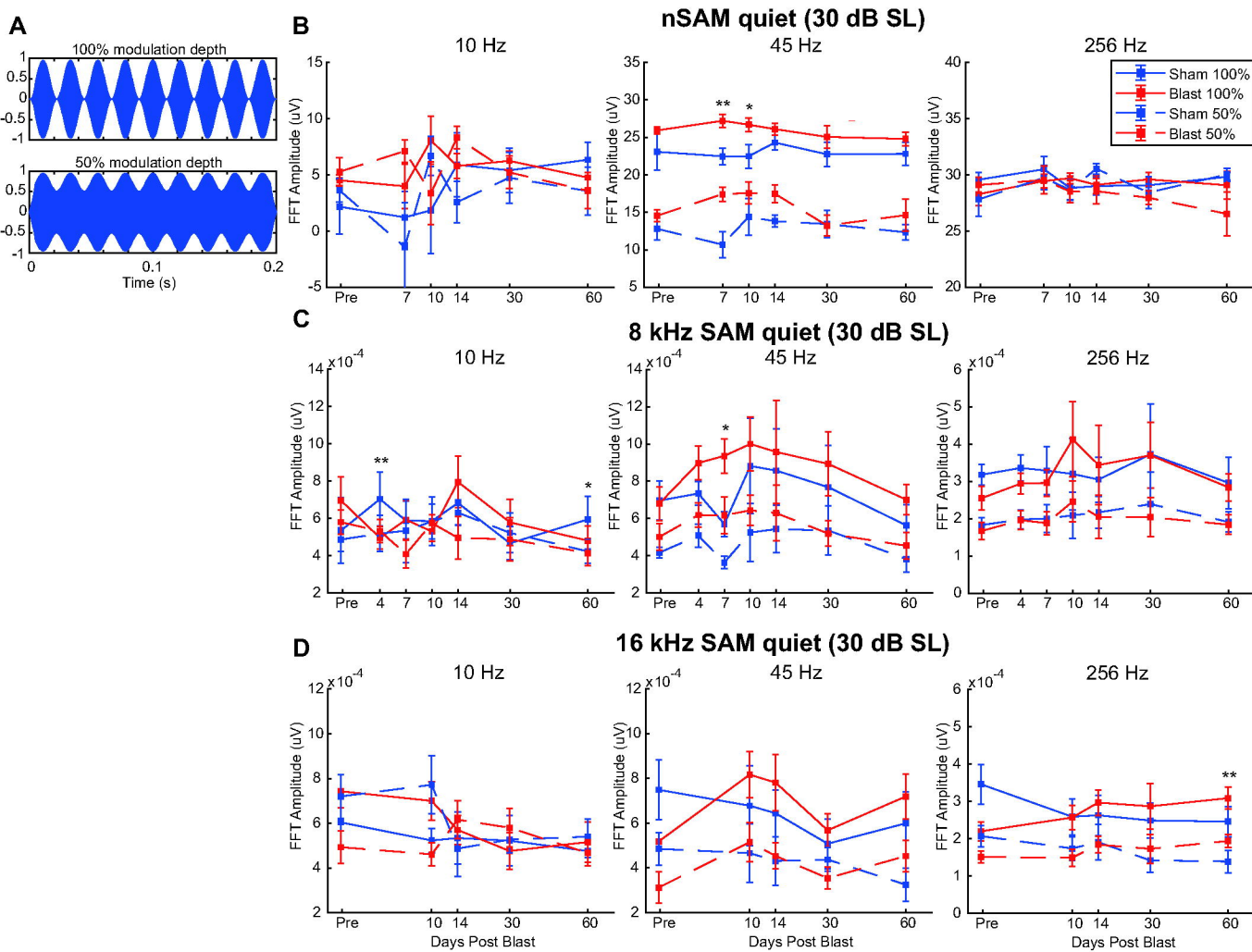
Supplementary Table 1. Simple main effects of Group on Click, 8 kHz and 16 kHz ABR threshold over time. Post-blast ABR thresholds of Blast (N=10) and Sham (N=6) groups are compared using rmANOVA at each time point recorded. A p<0.05 showed significant simple main effect of Group at that time point.



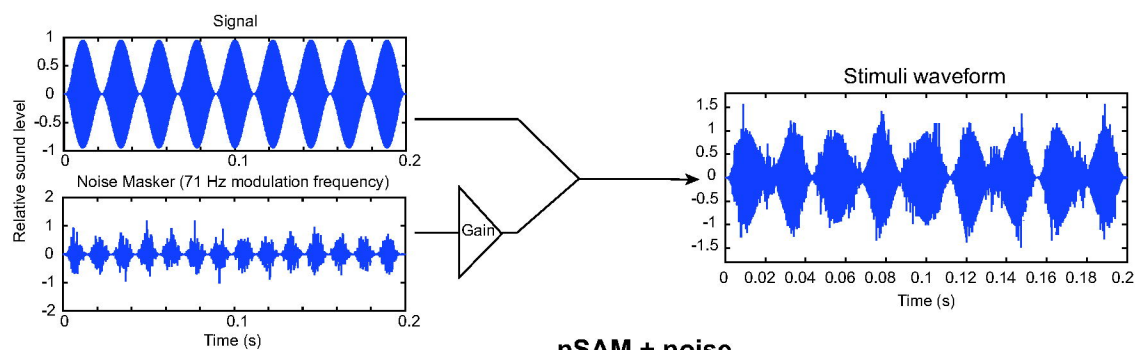




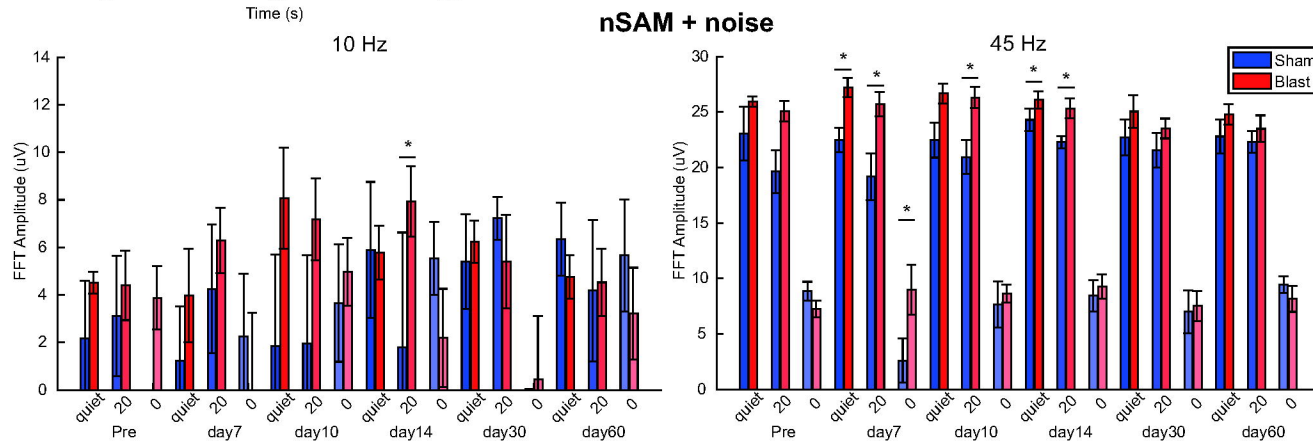




A



B



C

